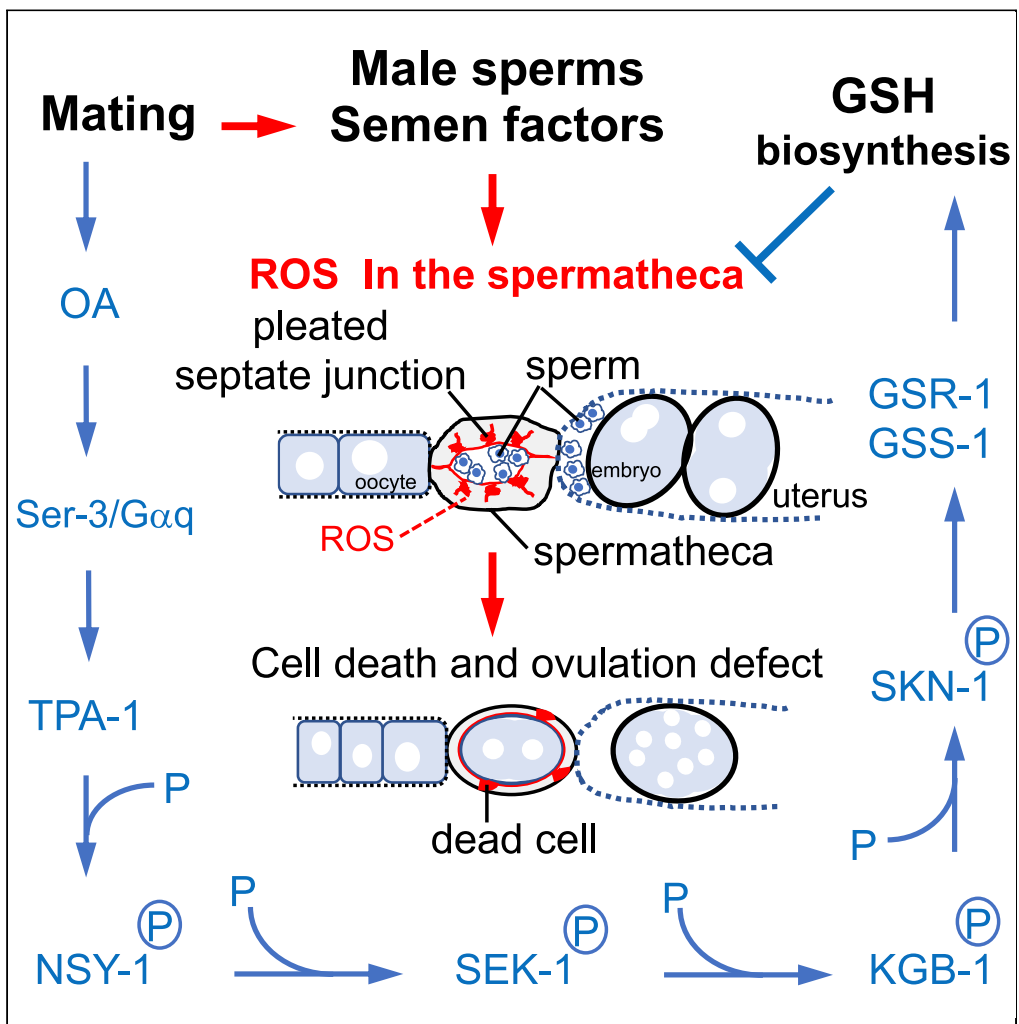


Article

Octopamine-MAPK-SKN-1 signaling suppresses mating-induced oxidative stress in *Caenorhabditis elegans* gonads to protect fertility



Yu Tsai, Yu-Chun Lin, Ying-Hue Lee

yinghue@gate.sinica.edu.tw

Highlights

Mating elicits oxidative stress and damages the spermathecal cells in hermaphrodites

This results in ovulation defects and suppresses the fertility of mated hermaphrodites

Octopamine (OA) counteracts the mating-induced damage to fertility in hermaphrodites

The OA-MAPK-SKN-1 signal cascade regulates GSH levels to reduce spermathecal ROS levels



## Article

Octopamine-MAPK-SKN-1 signaling suppresses mating-induced oxidative stress in *Caenorhabditis elegans* gonads to protect fertilityYu Tsai,<sup>1</sup> Yu-Chun Lin,<sup>1</sup> and Ying-Hue Lee<sup>1,2,\*</sup>

## SUMMARY

**Sexual conflict over mating is costly to female physiology. *Caenorhabditis elegans* hermaphrodites generally produce self-progeny, but they can produce cross-progeny upon successfully mating with a male. We have uncovered that *C. elegans* hermaphrodites experience sexual conflict over mating, resulting in severe costs in terms of their fertility and longevity. We show that reactive oxygen species (ROS) accumulate on the apical surfaces of spermathecal bag cells after successful mating and induce cell damage, leading to ovulation defects and fertility suppression. To counteract these negative impacts, *C. elegans* hermaphrodites deploy the octopamine (OA) regulatory pathway to enhance glutathione (GSH) biosynthesis and protect spermathecae from mating-induced ROS. We show that the SER-3 receptor and mitogen-activated protein kinase (MAPK) KGB-1 cascade transduce the OA signal to transcription factor SKN-1/Nrf2 in the spermatheca to upregulate GSH biosynthesis.**

## INTRODUCTION

Most animals reproduce sexually. For sexual animals to produce offspring, a successful mating event is necessary to transfer gametes before cross-fertilization can occur. A successful mating event generally involves physical contact between mating partners and the safe transfer of male sperm to female oocytes. Although mating is essential for reproduction, accumulating evidence reveals that successful mating can be both traumatic and damaging, potentially affecting adversely the physiologies of both sexes.

Mating typically involves aggressive and forceful physical contact between mating partners. Copulatory wounding (CW) and traumatic insemination (TI) are common in animals.<sup>1</sup> Both CW and TI may affect fitness, resulting in physiological and lifespan costs.<sup>2</sup> Females often suffer higher costs of CW and TI. For example, during mating of the nematode *Caenorhabditis elegans*, the male prods the hermaphrodite's vulva with sclerotized spicules, prying it open, before ejaculating sperm into the uterus.<sup>3</sup> Repetitive prodding with those spicules damages the cuticle surrounding the vulva, making them more vulnerable to pathogen infection.<sup>4,5</sup>

Male ejaculates contain sperm and seminal fluid, representing a complex cocktail of biologically potent substances such as nutrients, antioxidants, and hormones, which protect sperm viability and function and promote fertilization.<sup>6–8</sup> These substances may also exert behavioral and physiological impacts on females, altering their fecundity, immune response, and lifespan.<sup>9–11</sup> Many such impacts of seminal fluid on females have been revealed through studies on the fruit fly *Drosophila melanogaster*.<sup>5,12</sup> For example, the seminal fluid of *Drosophila* enhances egg-laying by females and reduces their desire to mate with other males.<sup>13,14</sup> These effects are beneficial from the male perspective but engender fitness and even lifespan costs for females.<sup>15,16</sup> Nevertheless, other studies have reported beneficial effects of semen for females. For example, factors in the seminal fluid of mammals recruit leukocytes and induce an inflammatory response in the female reproductive tract to defend against microbes in the uteri, thereby promoting sperm survival and zygote implantation.<sup>11,17</sup>

Thus, in animals, females incur higher mating costs than males, raising the question of whether this sexual conflict damages female fecundity and fertility and what measures females take to counteract those negative impacts. The former question has been addressed in studies using the multiple-mating approach in

<sup>1</sup>Institute of Molecular Biology, Academia Sinica, Taipei 115, Taiwan

<sup>2</sup>Lead contact

\*Correspondence: yinghue@gate.sinica.edu.tw  
<https://doi.org/10.1016/j.isci.2023.106162>



traumatically inseminating insects to compare the effects of single and multiple mating on fertility and longevity.<sup>18–21</sup> Those studies revealed that although multiple mating shortened female longevity, it had no adverse effect on their fertility. However, those conclusions were based on comparing single and multiple mating events but not between non-mating and mating. Hence, it remains unclear if the damaging impact of mating on fertility is attributable to the first mating event or if the first mating event already activates an adaptive mechanism to counteract the costs.

Here, we use *C. elegans* as a model to study the effects of mating cost on hermaphrodite sexual fitness at the genetic and molecular levels. We hypothesize that mating costs adversely affect hermaphrodite fitness. To secure and maximize their sexual reproductive fitness, hermaphrodites are likely to have evolved a protective system that counteracts those mating costs. There are two sexes in *C. elegans*, i.e., hermaphrodite and male.<sup>22</sup> Hermaphrodites produce both sperm and oocytes to reproduce and can also produce cross-progeny upon receiving sperm from males. This unique physiology is well suited to study the impact of mating costs on fertility since both non-mating and mating fertility can be assayed to determine accurately mating costs on fertility. Moreover, powerful genetic and molecular systems are already well developed for *C. elegans*, providing ample resources for manipulating and understanding the molecular mechanisms underlying any counteracting adaptations, if they exist, that might have evolved.

Our results show that mating elicits oxidative stress and damages the spermathecal bag cells, resulting in ovulation defects and consequently suppressing the fertility of mated hermaphrodites. To counteract this mating-induced damage to fertility, *C. elegans* hermaphrodites use the octopamine (OA)-mitogen-activated protein kinase (MAPK) signaling cascade to regulate transcription factor SKN-1/Nrf2 activity and increase antioxidant glutathione (GSH) levels after mating. Our findings provide strong molecular evidence for a protective mechanism against mating-induced damage to fertility and reveal the pivotal role of OA and GSH in protecting mating fertility.

## RESULTS

### Mating markedly increases fertility in young hermaphrodites

Under adequate food and a constant temperature of 22°C, we found that young N2 hermaphrodites can produce >250 self-offspring and produce >500 offspring after successfully mating with a young adult male (Figure 1A). Although mating activity promoted fertility, both survival rate and mean lifespan declined among mated hermaphrodites (Figure S1A), indicating that mated hermaphrodites experience stress. This result implies a trade-off between lifespan and the production of cross-progeny. However, it was unclear if this tradeoff is associated with a potential adverse effect of mating, a burden of doubled fertility, or both.

The non-mating fertility (self-fertility) of *C. elegans* hermaphrodites depends on the number of self-sperm produced. After successfully mating, hermaphrodites use both self-derived and male-contributed sperms for progeny production. Therefore, it is conceivable that, correlated with greater sperm availability, more offspring would be produced by mated hermaphrodites than unmated hermaphrodites if mating events do not negatively impact fertility. The vulva of *C. elegans* hermaphrodites is finely constructed with muscles and innervated by neurons, and it is essential for egg deposition.<sup>23</sup> However, during mating, males damage the cuticle surrounding the vulva by repetitive and forceful prodding with their tail spicules.<sup>4</sup> Accordingly, mated hermaphrodites may experience injury and, perhaps, some uncovered damages associated with mating, and we hypothesize that hermaphrodites likely evolved a protective system to counteract mating-associated harm and preserve their reproductive fitness so that optimal progeny production can still occur.

### OA secures mating-promoted fertility and protects hermaphrodites from mating-associated mortality

To determine if a mating-protective mechanism has evolved in hermaphrodites, we screened for genetic mutants that still produced self-offspring but did not significantly increase their offspring production after mating with young N2 males. When we examined mutant worms defective in the synthesis of bioamines, such as serotonin and dopamine (Figure 1B, upper panel), we found that the mated *tbh-1* and *tdc-1* null mutant hermaphrodites exhibited these phenotypes (Figure 1B, lower panel). In addition, these mutant hermaphrodites also exhibited reduced self-fertility compared to N2 hermaphrodites. The *tdc-1* and *tbh-1* genes encode key enzymes that catalyze the first and final steps, respectively, for metabolizing tyrosine into OA, the invertebrate counterpart of norepinephrine in vertebrates.<sup>24</sup> Because *tbh-1* mutant

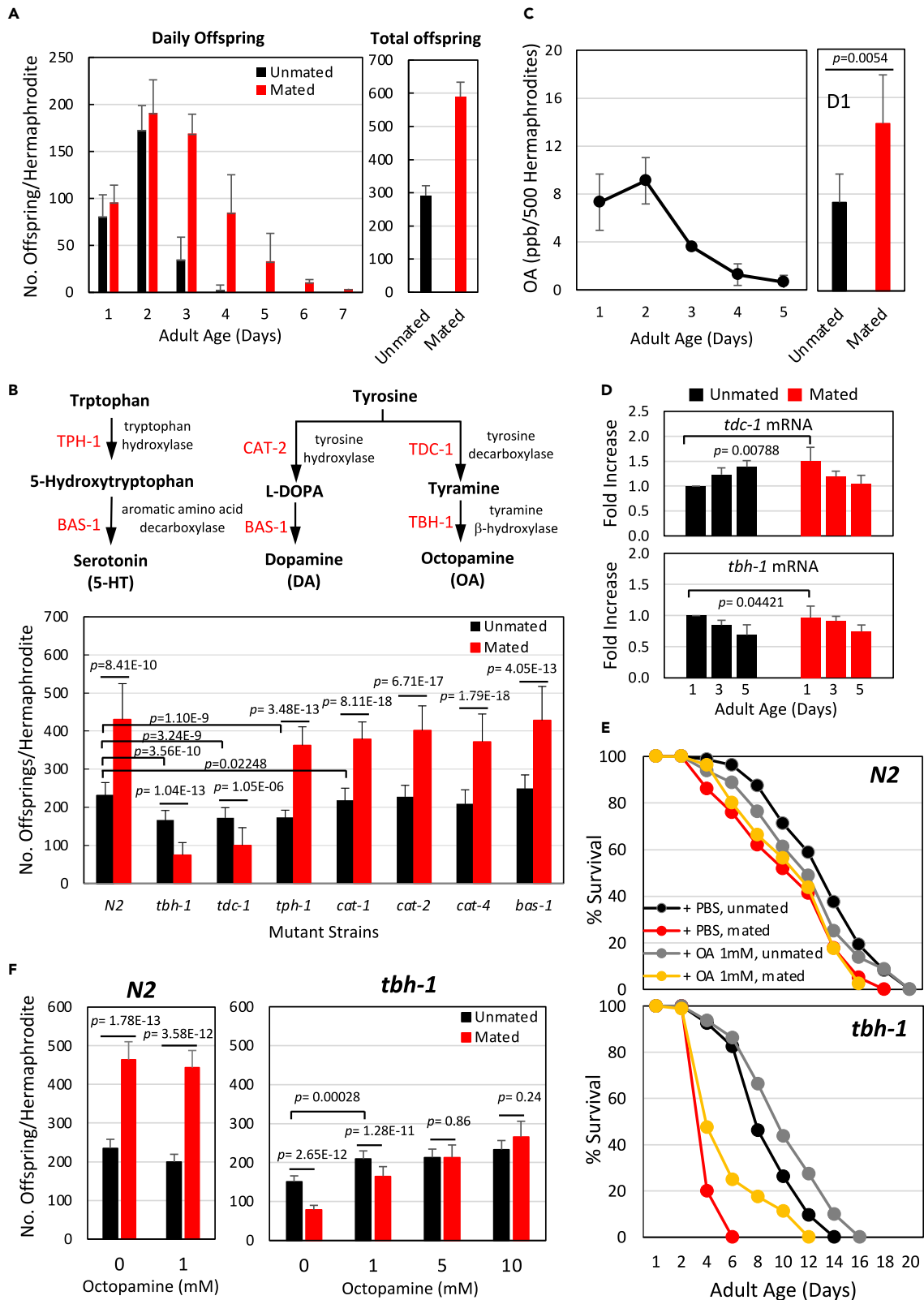


**Figure 1. Octopamine (OA) secures mating-promoted fertility and protects against mating-induced mortality in *C. elegans* hermaphrodites**

(A) Mating stimulates hermaphrodite fertility. Left panel, fertility was assayed by measuring daily offspring production by individual hermaphrodites at 22°C. Right panel, summation of daily offspring numbers from the left panel.  
 (B) Defects in OA synthesis abolish mating-stimulated fertility and inhibit basal fertility in hermaphrodites. Upper panel, flowchart illustrating the steps of bioamine synthesis and the enzymes involved. Lower panel, fertility assay on mutant hermaphrodites.  
 (C) Mating increases OA levels in hermaphrodites. OA samples from hermaphrodites of the indicated ages and groups were measured by UPLC/MS-MS, and their levels were calculated from the peak areas shown in Figure S1B.  
 (D) Mating increases the expression of *tdc-1* mRNA. Real-time qPCR of mRNA levels of *tdc-1* and *tbh-1* responsible for OA synthesis. Data represent mean  $\pm$  SD,  $n = 6$ .  $p$ -values were calculated using a two-tailed  $t$ -test.  
 (E) OA supplementation improves the survival rate and lifespan of mated *tbh-1* hermaphrodites. Hermaphrodites received 1 mM OA from the late L4 stage until day 5 of adulthood.  
 (F) OA supplementation improves the fertility of unmated *tbh-1* hermaphrodites and prevents suppressed fertility in mated *tbh-1* hermaphrodites. For B and F, fertility was assayed by measuring total offspring production by individual hermaphrodites at 22°C. Data represent mean  $\pm$  SD,  $n \geq 30$ .  $p$ -values were calculated using a two-tailed  $t$ -test. See also Figures S1 and S2.

nematodes are completely deficient in OA production compared to *tdc-1* mutants, we used the *tbh-1* mutant strain for subsequent experiments to study the role of OA in fertility.

First, we monitored OA levels among reproductive hermaphrodites. We detected the highest OA levels on day 2 (D2) among adult *N2* hermaphrodites, with levels declining rapidly thereafter with advancing age (Figure 1C, left panel; Figure S1B). This decline correlated well with diminished offspring production as hermaphrodites aged. On day 5 (D5), when self-fertility ceased, OA levels had decreased to  $\sim$ 10% of those of D2 levels. Mating appears to stimulate *tdc-1* expression and OA production. OA levels were significantly elevated in D1 mated hermaphrodites (Figure 1C, right panel), as were their *tdc-1* mRNA levels (Figure 1D).

Rather than promoting fertility, as observed for *N2* and other mutant hermaphrodites, mating markedly inhibits the fertility of both *tbh-1* and *tdc-1* hermaphrodites. Furthermore, lifespan monitoring revealed that mating significantly curtailed the lifespan of *tbh-1* hermaphrodites (Figure 1E, lower panel). These results indicate that *tbh-1* hermaphrodites experience severe stress upon being mated. We postulated that hermaphrodites produce OA to protect themselves from the adverse effects of mating and to secure mating-promoted fertility.

To test that supposition, we supplied OA to *tbh-1* hermaphrodites starting from the late L4 stage, i.e., when transferred to mate with *N2* adult males, until D5 of the adult stage when offspring production ceased. OA supplementation indeed improved the survival and extended the lifespan of both unmated and mated *tbh-1* hermaphrodites (Figure 1E). OA also improved self-fertility in unmated *tbh-1* hermaphrodites, and at a concentration  $>5$  mM, it abolished the inhibited offspring production in mated *tbh-1* mutant hermaphrodites (Figure 1F).

Although OA is essential to protect hermaphrodites and secure mating-promoted fertility, it is dispensable for males for their mating activities and sperm production. Young *tbh-1* mutant males sired as many offspring as *N2* males when mated with either *N2* or *tbh-1* hermaphrodites (Figure S1C).

TBH-1 is expressed in RIC neurons and the proximal gonad sheath (Figure S2A).<sup>25</sup> To establish if RIC-derived TBH-1 is the crucial source of OA that protects hermaphrodite fertility, we laser-ablated RIC neurons in L4 hermaphrodites carrying a GFP transgene driven by the *tbh-1* promoter (Figure S2B)<sup>25</sup> and then allowed them to mate and reproduce. Interestingly, ablation of RIC neurons did not abolish mating-promoted fertility (Figure S2C), indicating that OA from RIC neurons contributes minimally to this effect.

**OA deficiency causes defects in the exit of fertilized oocytes from spermathecae and delays ovulation**

To understand how OA deficiency affects the fertility of mated hermaphrodites, we examined oogenesis by labeling gonads of D1 hermaphrodites with EdU (5-ethynyl-2'-deoxyuridine) to monitor mitotic activity and nuclei motion. We found that the numbers of labeled nuclei and their migratory speed from the mitotic zone to the late pachytene region did not differ between the gonads of either mated or unmated *N2* and *tbh-1* hermaphrodites (Figure S2D).

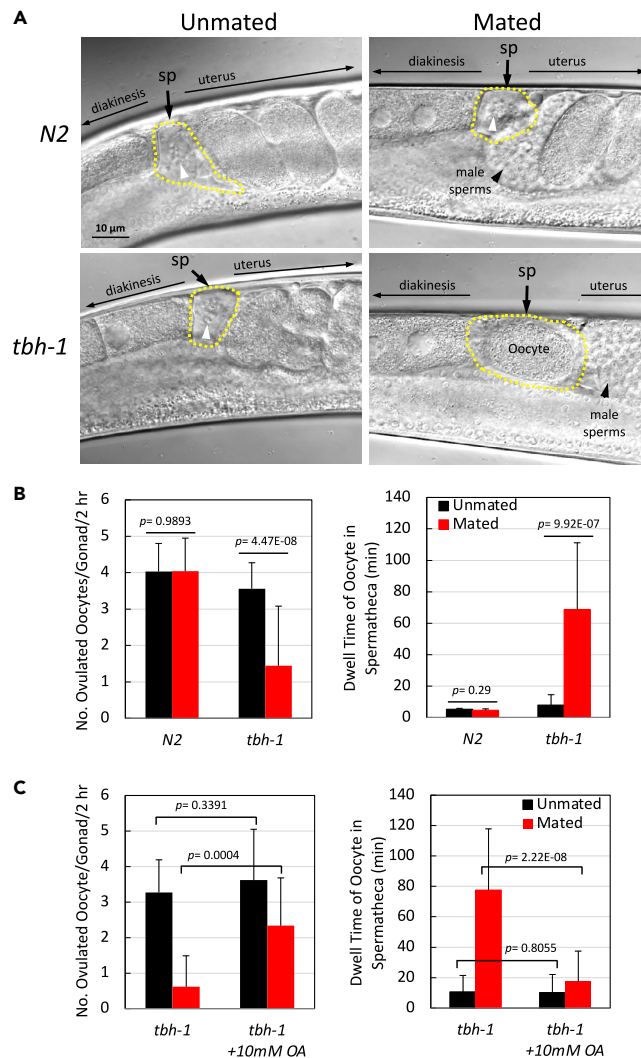


**Figure 2. OA deficiency causes ovulation defects in mated *C. elegans* hermaphrodites**

(A) OA deficiency induces spermathecal dilation in mated *tbh-1* hermaphrodites. Representative images of the spermathecae in mated and unmated *N2* and *tbh-1* hermaphrodites. White arrowheads indicate sperms inside spermathecae (denoted by "sp" and outlined with dotted lines).

(B) OA deficiency reduces the number of ovulated oocytes by prolonging their dwell time in spermathecae.

(C) OA supplementation shortens the dwell time of oocytes in spermathecae and rescues the number of ovulated oocytes in mated *tbh-1* hermaphrodites. For B and C, day 1 hermaphrodites were anesthetized and video-recorded under a microscope for 2 h (see example in Video S1). Numbers of oocytes ovulated (left panel) and their dwell time in the spermathecae (right panel) were quantified based on the video recordings. Data represent mean  $\pm$  SD,  $n \geq 20$  gonads.  $p$ -values were calculated using a two-tailed  $t$ -test. See also Figure S2 and Videos S1, S2, and S3.

Moreover, we examined ovulation and egg-laying activity. We observed that only fertilized oocytes from mated *tbh-1* hermaphrodites stalled in the spermathecae (resulting in dilated spermathecae) during fertilization and ovulation (Figure 2A; Video S1). Under anesthesia, a fertilized oocyte from an unmated *N2* or *tbh-1* hermaphrodite stayed in the spermatheca for 5 to 7 min (Figure 2B). However, in >85% of mated *tbh-1* hermaphrodites that we observed, once their mature oocytes entered the spermatheca, they often remained there for the entire 2-h observation time. Such stalled fertilized oocytes typically prevented subsequent oocytes from entering the spermatheca (Video S1). Nevertheless, we did observe a few successful exits of initially stalled fertilized oocytes from spermatheca, apparently pushed out by the preceding mature oocyte (Video S2). These abnormalities suggest a defect in the contractile activity of the spermathecae, but not of the proximal sheath cells surrounding mature oocytes, in mated *tbh-1* mutant hermaphrodites.

Because OA supplementation effectively rescued the bolstered mating-induced fertility of *tbh-1* hermaphrodites, we examined if OA supplementation could also rescue their ovulation defects. Indeed, OA supplementation (10 mM) was sufficient to significantly reduce stalling of fertilized oocytes in spermathecae during ovulation of most mated *tbh-1* hermaphrodites (Figure 2C; Video S3). These results clearly demonstrate that mating exerts adverse effects on the spermathecae of *tbh-1* hermaphrodites to disrupt coordinated and timely ovulation and that OA can prevent these defects.

### OA regulates ovulation via the G protein-coupled receptor, SER-3, and the JNK-like MAPK KGB-1 signaling pathway

To reveal how OA prevents mating-associated defects in ovulation and secures mating-promoted fertility, we again screened genetic mutants for receptors and downstream factors that mediate OA signaling and function. *C. elegans* possesses three known OA receptors, i.e., OCTR-1, SER-3, and SER-6.<sup>26,27</sup> Like *tbh-1* mutant hermaphrodites, mating significantly inhibits fertility in mutant hermaphrodites carrying the *ser-3* null allele, whereas, as in wild-type, it greatly promotes fertility in mutant hermaphrodites with either of the *ser-6* and *octr-1* or both alleles (Figure 3A). SER-3 is expressed in several structures, including numerous neurons, head muscles, and hermaphrodite gonads where it is expressed more strongly in the spermathecae.<sup>28</sup>

SER-3 is a G protein ( $G\alpha$ )-coupled receptor. Notably, mutant hermaphrodites carrying a defective allele of *egl-30* encoding  $G\alpha$  exhibit diminished offspring production when mated (Figure 3B). We also examined several other  $G\alpha$ -coupled neurotransmitter receptors, including dopamine and other serotonin receptors, but none appeared to mediate the impact of OA on fertility (Figure S3A). It has been reported previously that protein kinase A (PKA) mediates the action of  $G\alpha$ -coupled neuromodulator receptors on synaptic and cellular functions,<sup>29</sup> but we did not uncover any role for PKA in OA signaling (Figure S3B).

Next, we screened for candidate factors downstream of the SER-3 and  $G\alpha$  signaling pathway to better understand the OA regulatory mechanism (Figures S3 and S4). All identified mutant hermaphrodites that exhibited suppressed fertility upon mating are summarized in Figure 3B, displaying a similar phenotype to that observed for mated *tbh-1* hermaphrodites and together revealing a unique signaling pathway highly responsible, if not solely, for how OA acts on fertility upon mating. In this pathway, OA signals to the  $G\alpha$ -coupled SER-3 receptor, which transduces the signal to a protein kinase C (TPA-1) and subsequently to an MAPK cascade involving MAP3K NSY-1, MAP2K SEK-1, and the JUN-like MAPK KGB-1. We also established that the ovulation defects we described above for *tbh-1* hermaphrodites also exist in these newly identified mutant hermaphrodites (data not shown).

To verify the pathway, we analyzed the activation pattern of KGB-1 in all identified mutant hermaphrodites using antibodies against KGB-1 and its phosphorylated form that indicates activation.<sup>30</sup> In response to mating, N2 hermaphrodites displayed enhanced levels of KGB-1 phosphorylation, with the highest levels occurring 8 h post-mating but gradually diminishing thereafter (Figure 3C). Accordingly, we examined KGB-1 phosphorylation levels in mated mutant hermaphrodites 8 h post-mating. As shown in Figure 3D, although basal levels of KGB-1 phosphorylation varied among different mutants, mating did not promote KGB-1 phosphorylation in any of these mutant hermaphrodites (unlike for N2 hermaphrodites), confirming that OA can signal to KGB-1 via SER-3, TPA-1, and the MAPK cascade in response to mating.

### SKN-1 is a downstream effector of JUN-like MAPK KGB-1 signaling and prevents mating-associated ovulation defects

KGB-1 promotes longevity and reproduction by regulating the expression of genes essential in stress responses and protein biosynthesis. For example, KGB-1 regulates the expression of numerous AP-1 (activator protein 1)-responsive genes during stress by controlling the activation of members of the AP-1 complex, such as JUN-1.<sup>31</sup> AP-1 is a pivotal transcription factor that regulates a wide range of cellular processes, including cell growth and proliferation.<sup>32</sup> Together with DAF-16, the KGB-1/AP-1 signaling axis promotes longevity.<sup>33</sup> Accordingly, we examined if DAF-16 and AP-1 components acted as effectors of the OA-MAPK KGB-1 signaling contributing to nematode fertility. Although mating-promoted fertility still occurred in *daf-16* null mutant hermaphrodites, it was absent from *jun-1* mutant hermaphrodites (Figure 4A). However, *jun-1* mutant hermaphrodites produce very few offspring, so our assay system may not have captured any effect. We also tested another AP-1 complex member, ATF-7, which is also regulated by MAPK signaling. Like DAF-16, ATF-7 did not appear to be involved in the impact of OA on mating fertility.



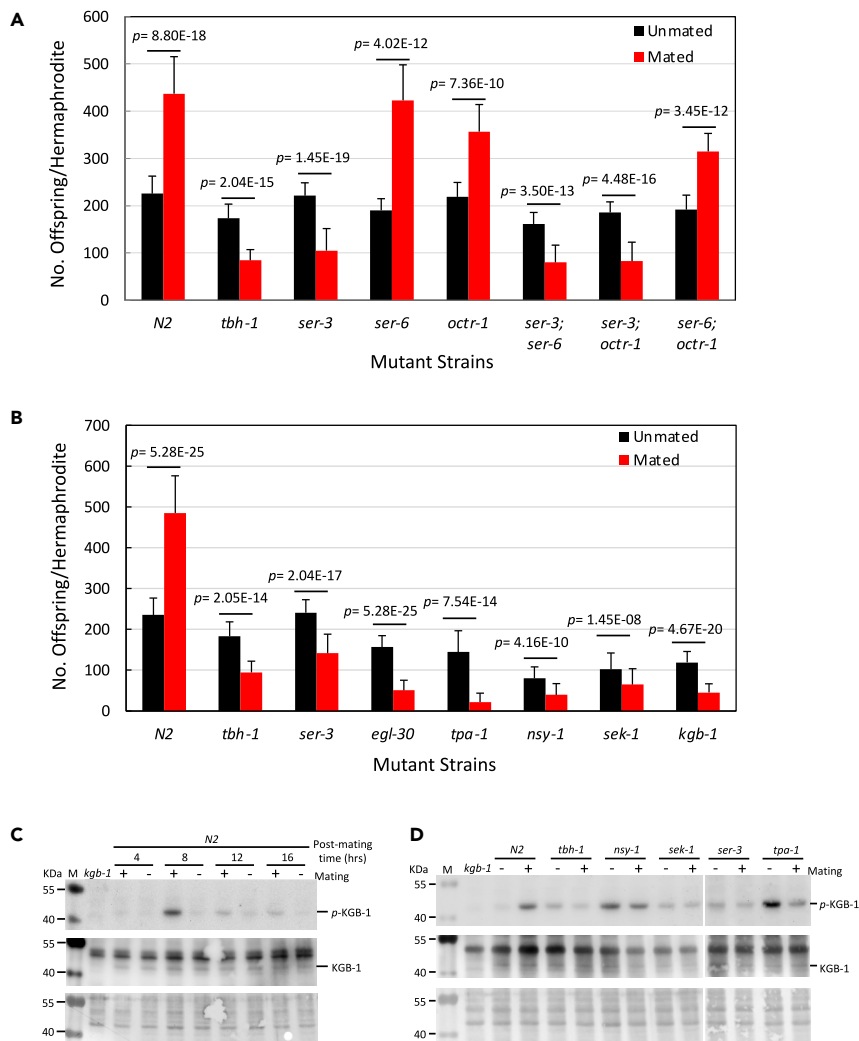


**Figure 3. OA signals the MAPK KGB-1 cascade via the SER-3 receptor to maintain mating-promoted fertility in *C. elegans* hermaphrodites**

(A) The SER-3 receptor mediates OA signaling to maintain mating-promoted fertility in hermaphrodites. (B) TPA-1 and the MAPK cascade transmit the OA signal to maintain mating-promoted fertility in hermaphrodites. These factors had been identified from our primary screening (Figures S3 and S4). Fertility was assayed by measuring total offspring production by individual hermaphrodites at 22 C. Data represent mean  $\pm$  SD,  $n \geq 30$ . p-values were calculated using a two-tailed t-test.

(C) Mating rapidly increases KGB-1 phosphorylation.

(D) Mating-induced KGB-1 phosphorylation is abrogated in all tested mutant hermaphrodites. For C and D, KGB-1 phosphorylation was analyzed by western blotting. Top and middle blots show phosphorylated KGB-1 and total KGB-1 signals, respectively. Bottom blot shows the corresponding Coomassie blue-stained loaded proteins. See also Figures S3 and S4.

KGB-1 regulates the expression of genes responsible for ribosomal biogenesis and translation that are essential for promoting reproduction.<sup>31</sup> Therefore, we assayed global protein biosynthesis activity in all identified mutant hermaphrodites. Interestingly, mating did not affect global protein synthesis in control N2 hermaphrodites, but it did enhance it in *tbh-1* and several other mutant hermaphrodites, including *kgb-1* (Figure S4D), indicating that OA to MAPK signaling does not act on protein synthesis to affect mating fertility.

SKN-1 is another anti-stress and longevity-promoting transcription factor that serves as an effector downstream of diverse signaling pathways, including MAPK PMK-1/p38 and insulin/insulin growth factor



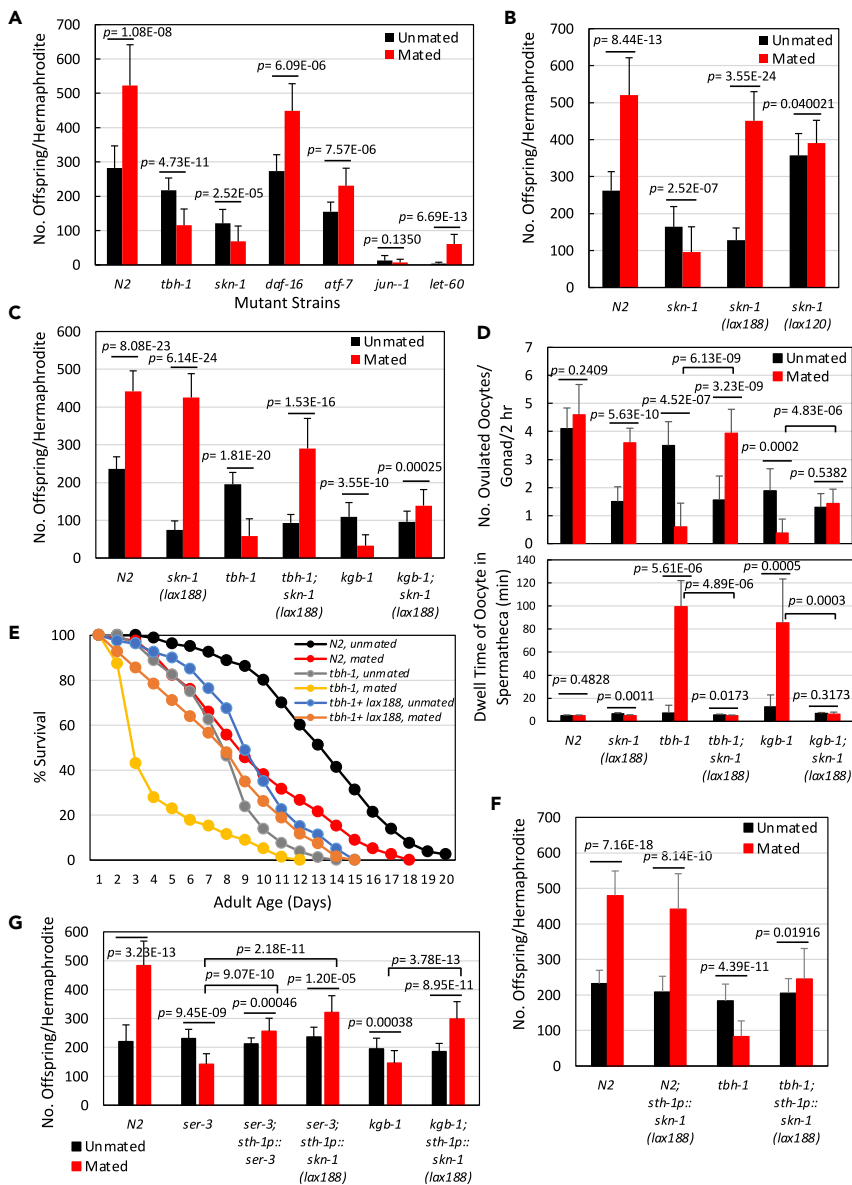


**Figure 4. SKN-1 is the downstream effector of OA-MAPK signaling to maintain mating-promoted fertility in *C. elegans* hermaphrodites**

(A) Effect of mating on hermaphrodite fertility for different mutant strains.

(B) Effect of *skn-1* gain-of-function alleles on self- and mating-based fertility.

(C) The *skn-1(Lax188)* allele rescues mating fertility in *tbh-1* and *kgb-1* hermaphrodites.

(D) The *skn-1(Lax188)* allele shortens the spermathecal dwell time of oocytes and recovers the number of ovulated oocytes in mated *tbh-1* and *kgb-1* hermaphrodites. Day 1 hermaphrodites were anesthetized and video-recorded under a microscope for 2 h, as shown in Video S1. The number of oocytes ovulated (left panel) and their spermathecal dwell time (right panel) were quantified based on the video recordings. Data represent mean  $\pm$  SD,  $n \geq 20$  gonads. p-values were calculated using a two-tailed t-test.

(E) The *skn-1(Lax188)* allele improves the survival rate and lifespan of mated *tbh-1* hermaphrodites.

(F) Specific expression of SKN-1(Lax188) in spermathecae abolishes the inhibited fertility displayed by mated *tbh-1* hermaphrodites.

(G) Spermatheca-specific expression of SER-3 and/or SKN-1(Lax188) abolishes the inhibited fertility displayed by mated *ser-3* and *kgb-1* hermaphrodites. For A-C and F-G, fertility was assayed by measuring total offspring production by individual hermaphrodites at 22°C. Data represent mean  $\pm$  SD,  $n \geq 30$ . p-values were calculated using a two-tailed t-test. See also Figure S5A, and Videos S4 and S5.

(IGF)-1-like DAF-16/FOXO.<sup>34,35</sup> Although, to our knowledge, SKN-1 has not been reported previously as mediating MAPK KGB-1 signaling, we observed that, like *tbh-1* mutant hermaphrodites, loss-of-function *skn-1* mutant hermaphrodites exhibited suppressed fertility upon mating (Figure 4A), implying an effector role for SKN-1 in the impact of OA-MAPK signaling on mated fertility.

We deployed two dominant and constitutively active *skn-1* alleles (*skn-1*[[*lax120*] and *skn-1*[[*lax188*]])<sup>36</sup> to validate that SKN-1 acts downstream of KGB-1 to mediate the effects of OA on ovulation and fertility. First, we assayed self and mated fertility in hermaphrodites carrying the *skn-1*(*lax120*) or *skn-1*(*lax188*) allele. Self-fertility of the *skn-1*(*lax120*) and *skn-1*(*lax188*) hermaphrodites differed significantly relative to that of *N2* hermaphrodites, with *skn-1*(*lax120*) hermaphrodites exhibiting a 36% increase, whereas *skn-1*(*lax188*) hermaphrodites displayed a 52% reduction. However, upon mating, *skn-1*(*lax188*) hermaphrodites produced 3.5-fold more cross-offspring than self-offspring, but *skn-1*(*lax120*) hermaphrodites only produced 9% more cross- than self-offspring (Figure 4B).

Because the *skn-1*(*lax188*) allele markedly increases mating-promoted fertility, we introduced it into *tbh-1* and *kgb-1* mutant hermaphrodites by crossing to assess if it could rescue their ovulation defects and improve their mating fertility. Indeed, as shown in Figure 4C, not only did the introduction of the *skn-1*(*lax188*) allele successfully counteract suppressed fertility in mated *tbh-1* and *kgb-1* mutant hermaphrodites but it also further secured their mating-promoted fertility (with a more pronounced effect in the *tbh-1* than *kgb-1* hermaphrodites). Moreover, it effectively eliminated the ovulation defect evident in the spermathecae of mated *tbh-1* and *kgb-1* mutant hermaphrodites (Figure 4D; Video S4) and greatly extended the lifespan of mated *tbh-1* mutant hermaphrodites (Figure 4E).

Furthermore, we used the 1.5 kb spermatheca-specific *sth-1* promoter<sup>37</sup> to drive the expression of the *skn-1*(*lax188*) allele specifically in spermathecae (Figure S5A). Spermatheca-specific expression of *skn-1*(*lax188*) effectively abolished the ovulation defect displayed by mated *tbh-1* mutant hermaphrodites and prevented fertility suppression (Figure 4F; Video S5), though spermatheca-specific *skn-1*(*lax188*) did not restore mating fertility to the levels detected for ubiquitous expression of *skn-1*(*lax188*) in mated *tbh-1* hermaphrodites (Figure 4C), implying that optimal mating fertility requires OA signaling and SKN-1 function in other tissues.

Lastly, to further confirm our findings of the OA signaling pathway on mating fertility, we again expressed SKN-1(*lax188*) driven by the *sth-1* promoter in *ser-3* and *kgb-1* hermaphrodites to see if the spermatheca-specific *skn-1*(*lax188*) can abolish the inhibited fertility in both mated *ser-3* and *kgb-1* hermaphrodites as in *tbh-1* hermaphrodites. Indeed, spermatheca-specific *skn-1*(*lax188*) effectively abolish the inhibited fertility in both mated *ser-3* and *kgb-1* hermaphrodites (Figure 4G), supporting that the SER-3-KGB-1 pathway is the major, if not solely, signal pathway to mediate OA regulation on ovulation in the spermatheca.

Taken together, we have identified SKN-1 as the downstream effector of KGB-1 in the mating-activated OA-MAPK signaling pathway that protects ovulation activity and the mating-promoted fertility in hermaphrodites.

### SKN-1 mitigates mating-enhanced levels of reactive oxygen species (ROS) in spermathecae by maintaining glutathione homeostasis

SKN-1, the nematode ortholog of human Nrf2, promotes anti-stress responses and extends lifespan.<sup>38</sup> SKN-1/Nrf2 exerts an essential role in antioxidative stress, controlling the transcription of antioxidant enzymes such as superoxide dismutase (SOD) and glutathione S transferase.<sup>39–41</sup> Accordingly, we assessed oxidative stress and ROS localization in mated *tbh-1* mutant hermaphrodites using a ROS-reactive fluorogenic probe (CellROX orange, Molecular Probes) to detect ROS in live worms. As an ROS-positive reference strain, we adopted DAF-16-deficient adult hermaphrodites since they display severe oxidative stress in many cell types, including neurons and intestinal cells. Surprisingly, we did not detect clear ROS signals in *tbh-1* mutant hermaphrodites, unlike DAF-16-deficient hermaphrodites that, as anticipated, exhibited strong ROS signals in the intestine and muscles (Figure S5B). Instead, a faint and barely distinguishable ROS signal appeared in the spermathecae of unmated hermaphrodites (Figure S5B). Interestingly, mating strongly enhanced ROS signal in the spermathecae of *tbh-1* mutant hermaphrodites but not in *N2* hermaphrodites (Figures 5A, S5C, and S6A). These ROS signals were concentrated at the apical surface of bag cells in the spermathecal lumen (Figure 5B).

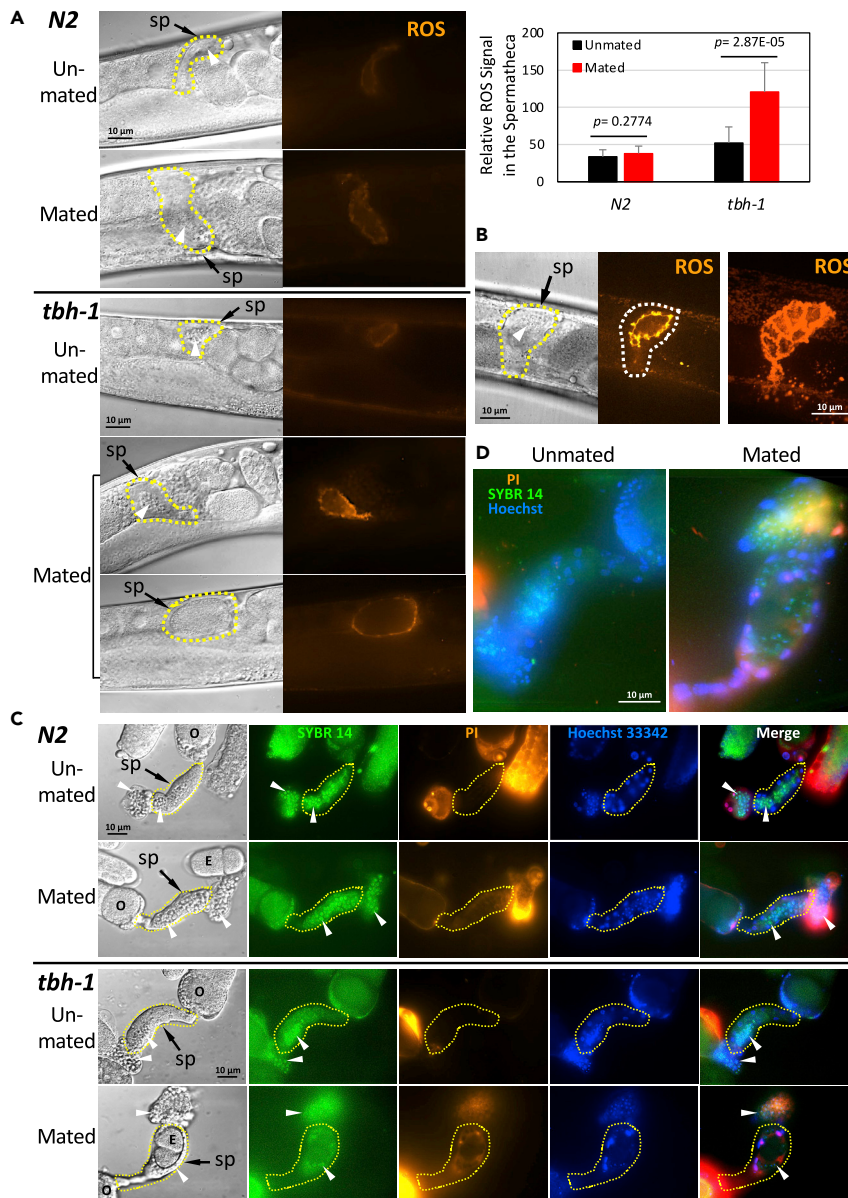


**Figure 5. Mating enhances ROS signal on the apical surface of *C. elegans* spermathecae and causes cell death in the spermathecae of mated *tbh-1* mutant hermaphrodites**

(A) ROS signals are enhanced solely in the spermathecae of mated *tbh-1* mutant hermaphrodites. Dilated spermathecae are common in mated *tbh-1* mutant hermaphrodites. Left panel, DIC and fluorescent images of the spermathecae of day 1 adult hermaphrodites. Right panel, relative levels of spermathecal ROS signal quantitated from images in Figure S6A using ImageJ. Data represent mean  $\pm$  SD,  $n = 10$ . *p*-values were calculated using a two-tailed *t*-test.

(B) Mating-enhanced ROS localize on the apical surface of the spermathecae of mated *tbh-1* mutant hermaphrodites. The left panel shows one of the image series. Right panel, 3D image of ROS in the spermathecae, constructed from the same image series.

(C) 3D images of the *tbh-1* spermathecae shown in (C, lower part). Images of serial sections from the same *tbh-1* spermathecae were used to construct the 3D image. Spermathecae are outlined by dotted circles. White arrowheads indicate sperms. E, embryo; O, oocyte; PI, propidium iodide; sp, spermatheca. See also Figures S5 and S6.

(D) Mating induces death of spermathecal bag cells in *tbh-1* mutant hermaphrodites. Fluorescent images of the spermathecae of day 1 adult hermaphrodites are shown.

This enhanced ROS signal on the apical surface of spermathecal bag cells raises the possibility that they and the sperm they contain may be targeted and damaged. Accordingly, we examined the viability of bag cells and their encased sperm inside the spermathecae of mated *tbh-1* hermaphrodites. Indeed, compared to those of mated *N2* and unmated *tbh-1* hermaphrodites, the bag cells of mated *tbh-1* hermaphrodites were more permeable to propidium iodide (PI), a molecule that cannot cross living cell membranes. Moreover, the nuclei of numerous bag cells were readily stained by PI, indicating that the spermathecal membrane of mated *tbh-1* hermaphrodites had been damaged, subsequently inducing cell death (Figures 5C and 5D). In contrast, the viability of sperms encased by bag cells and those located in the uteri near the spermatheca-uterus junction appeared unaffected (Figure 5C, SYBR 14-stained).

Together, these results indicate that mating can increase ROS levels and damage bag cells in the spermatheca. Thus, we postulated that the OA-MAPK-SKN-1 signaling cascade activated upon mating might suppress ROS generation to protect spermathecal function. Accordingly, we examined the roles of SKN-1/Nrf2-regulated antioxidant enzymes (catalases and SODs) in mating fertility. However, unlike *tbh-1* hermaphrodites, mated mutant hermaphrodites lacking SOD or catalase activity still displayed mating-promoted fertility (Figures S7A and S7B), indicating that these enzymatic antioxidants are not involved in how the OA-MAPK-SKN-1 signaling cascade contributes to mating fertility.

The reduced form of glutathione, GSH, is a tripeptide molecule and the most abundant antioxidant in cells, either intracellularly or extracellularly. GSH, together with glutathione peroxidases (GPXs) and transferases (GSTs), plays a major role in redox homeostasis, antioxidant defense, and detoxification.<sup>42,43</sup> SKN-1/Nrf2 regulates GSH levels by controlling the transcriptional expression of *gcs-1* that encodes for GCS-1, the first enzyme acting in the biosynthesis of GSH from glutamine and cysteine.<sup>40</sup> However, mRNA levels of *gcs-1* in whole-nematode lysates were not reduced in *tbh-1* mutant hermaphrodites relative to *N2*, regardless of mating status (Figure S7C). Instead, we found that the mRNA levels of *gss-1* and *gsr-1* decreased by 30% and 25%, respectively, in the *tbh-1* mutants relative to *N2* hermaphrodites (Figure S7C). GSS-1 (glutathione synthetase) catalyzes the second and final step of GSH biosynthesis, whereas GSR-1 (glutathione reductase) reduces the oxidized form of glutathione (GSSG) back to GSH. Both enzymes are important in maintaining GSH levels and the GSH/GSSG ratio. Accordingly, we hypothesized that GSH levels might be compromised in mated *tbh-1* mutant hermaphrodites. Indeed, although levels of total glutathione were not significantly reduced in unmated *tbh-1* mutant hermaphrodites relative to *N2*, only in the *tbh-1* hermaphrodites did mating substantially curtail total glutathione levels (Figure 6A, left panel). Furthermore, mating also depleted GSH levels more significantly in *tbh-1* than in *N2* hermaphrodites (Figure 6A, right panel), indicating that the antioxidant capacity of glutathione is reduced substantially in mated *tbh-1* hermaphrodites.

To test if glutathione plays a pivotal role in protecting nematodes against the mating-associated ROS that suppresses fertility, we supplied GSH to hermaphrodites, starting from mating setup until they finished egg-laying, and then assayed them for their fertility. Although GSH supplementation at 5 or 10 mM did not further increase mating-promoted fertility in *tbh-1* hermaphrodites to the levels observed for mated *N2* hermaphrodites, it still effectively prevented fertility from being suppressed (Figure 6B). In contrast, supplementation with other potent antioxidants, N-acetyl-L-cysteine (NAC), L-ascorbic acid, melatonin, and  $\alpha$ -lipoic acid did not counteract fertility suppression in mated *tbh-1* hermaphrodites (Figures S7D–S7G). Moreover, GSH supplementation also reduced ROS signal and prevented stalling of fertilized oocytes in the spermathecae of mated *tbh-1* mutant hermaphrodites (Figures 6C and 6D; Figure S6B and Video S6). GSH is the substrate for GPXs and GSTs to maintain redox homeostasis.<sup>42,43</sup> Currently, *C. elegans* has 8 GPX and 44 GST isoforms (Wormbase), of which *gst-4* and *gst-10* were reported as the target genes of SKN-1.<sup>44</sup> While several GPXs are extracellular, all GSTs are located in the cytosol and thus less likely involved in the OA-regulated ROS reduction in the spermathecal lumen. Nevertheless, we examined the effect of each GPXs and these two SKN-1-targeted GSTs on mating fertility. Figure S7H shows that defects in individual GPXs and GSTs do not inhibit fertility in mated hermaphrodites.

Together, these results indicate that glutathione is likely the primary antioxidant protecting nematodes from mating-induced ROS in the spermathecae and that it maintains ovulatory function.

## DISCUSSION

That mating engenders costs to females is not uncommon among animals that undertake sexual reproduction, but those costs may be concealed by adaptive systems that have evolved to offset any detrimental

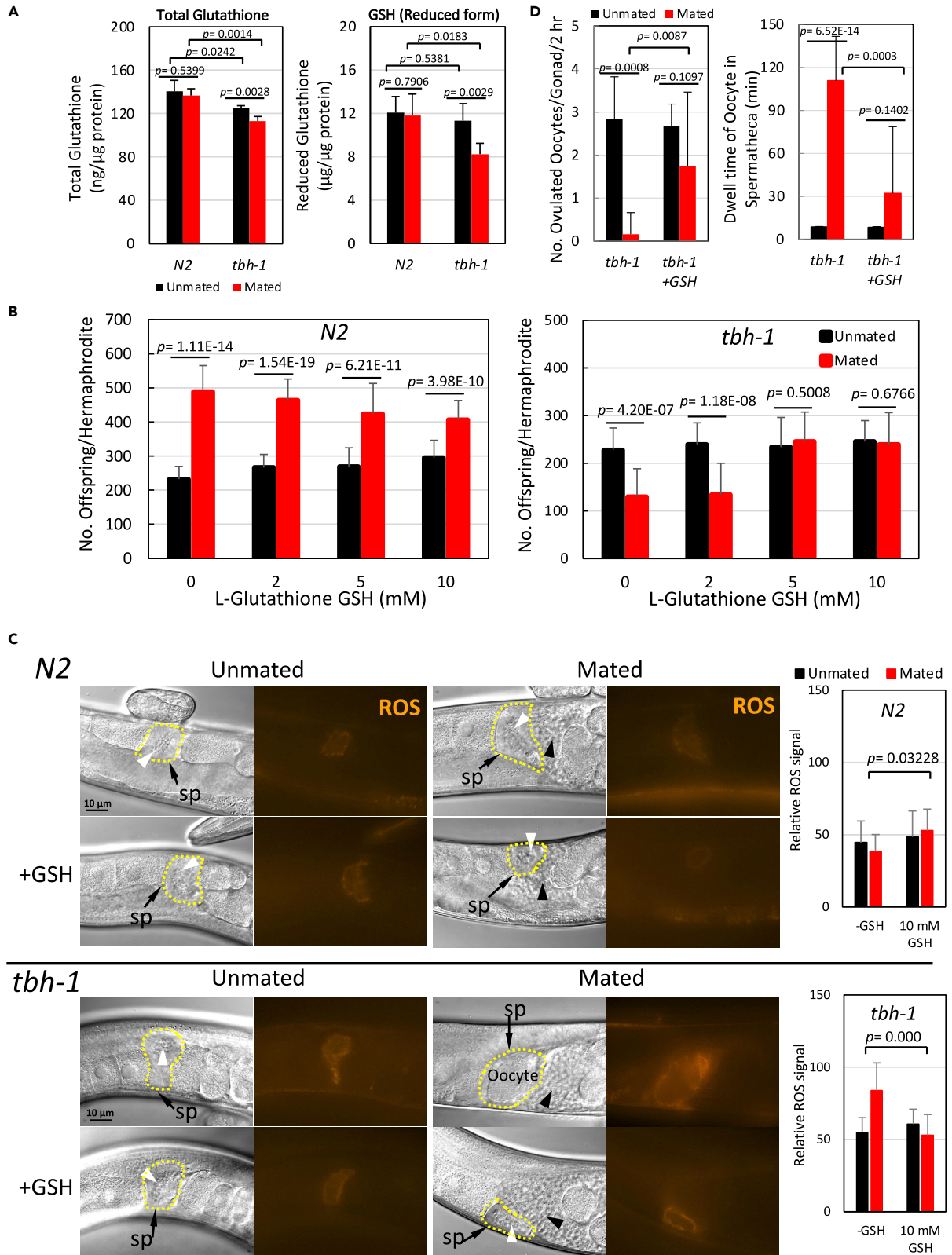




**Figure 6. OA deficiency reduces glutathione biosynthesis, and glutathione supplementation ameliorates the mating-stimulated ROS production and suppressed fertility displayed by mated *tbh-1* mutant *C. elegans* hermaphrodites**

(A) Total and reduced glutathione levels in mated *tbh-1* mutant hermaphrodites. Left and right panels show total glutathione and reduced glutathione levels, respectively. Data represent mean  $\pm$  SD of three independent experiments. p-values were calculated using a two-tailed t-test.

(B) Glutathione supplementation prevents the suppressed fertility displayed by mated *tbh-1* hermaphrodites. Fertility was assayed by measuring total offspring production by individual hermaphrodites. Data represent mean  $\pm$  SD,  $n \geq 30$ . p-values were calculated using a two-tailed t-test.

(C) Glutathione supplementation reduces the ROS signal in spermathecae of mated hermaphrodites. Left panel and middle panels, DIC and fluorescent images of the spermathecae of day 1 adult hermaphrodites. Right, relative levels of spermathecal ROS signal quantitated from images displayed in Figure S6B using ImageJ. Data represent mean  $\pm$  SD,  $n = 10$ . p-values were calculated using a two-tailed t-test.

(D) Glutathione supplementation improves the ovulation rate and reduces the spermathecal dwell time of oocytes of mated *tbh-1* hermaphrodites. The number of oocytes ovulated (left panel) and their spermathecal dwell time (right panel) were quantified based on video recordings. Data represent mean  $\pm$  SD,  $n \geq 20$ . p-values were calculated using a two-tailed t-test. White arrowheads indicate sperm inside spermathecae (denoted "sp" and outlined by dotted lines), and dark arrowheads indicate male sperm in the uterus. See also Figures S6 and S7, and Video S6.

effects. Here, we show that mating in nematodes impairs ovulation by enhancing ROS formation on the apical membrane of spermathecal bag cells, eliciting cell damage. However, we have discovered that these nematodes have evolved a protective system involving the OA-MARK signaling cascade that upregulates SKN-1/Nrf2 activity, which promotes glutathione biosynthesis and effectively abolishes mating-induced ROS in the spermathecae.

The mating-induced ROS in the lumen of spermatheca is likely attributable to the male ejaculate that contains sperm and seminal substances. Apart from their destructive effects, it is well established that ROS at biological levels acts as a signaling molecule to control cellular processes.<sup>45</sup> Mammalian spermatozoa are highly vulnerable to oxidative stress due to their unique physical structure and biochemical composition. However, their ability to capacitate for successful fertilization is redox-regulated and therefore requires a low level of ROS in semen to stimulate capacitation.<sup>46</sup> Thus, spermatozoa themselves generate ROS. Moreover, mammalian seminal fluid contains endogenous ROS principally from immature and dead spermatozoa.<sup>47</sup> Immature sperm can produce excessive ROS due to their abnormal oxidation activity in mitochondria, and dead sperms release enzymes such as L-amino acid oxidase and NADPH oxygenase that oxidize seminal substances and sperm debris to generate peroxide.<sup>46,48</sup> Dead sperms may also exist in the *C. elegans* ejaculate to fuel ROS overproduction. In addition, sperms of male *C. elegans* are larger and take precedence over hermaphroditic sperms to fertilize oocytes.<sup>49</sup> Though it remains to be tested, it is tempting to postulate that male sperms may produce more ROS than hermaphroditic sperms due to their greater size and superior strength in competing for oocytes. Regardless of the ROS source following mating, the surge in ROS must disrupt antioxidant homeostasis in the gonad, thus necessitating GSH activity to prevent any pathological effects. Interestingly, the mating-enhanced ROS specifically targets the apical side of spermathecal bag cells and not sperms, proximal oocytes, the oviduct sheath, or uteri. One possible explanation for this specificity is the unique membrane structure of bag cells that, uniquely among somatic gonad cells, possesses heavily pleated septate junctions that undergo repetitive unzipping and zipping in accordance with ovulation cycles.<sup>50</sup> Therefore, the membranes on bag cell apical surfaces must be very fluid and extremely rich in polyunsaturated fatty acids, rendering them highly susceptible to ROS attack and lipid peroxidation.

Although the gonads of *tbh-1* mutant hermaphrodites lack OA protection, their pro- and antioxidant systems must still display homeostasis so that essential oxidation activity can occur without impairing the spermathecal ovulation necessary for self-progeny production. However, this balance is perturbed by mating activity that results in exposure to male sperms and seminal substances, leading to higher levels of ROS and pathological changes in the reproductive tract of hermaphrodites and consequently impairing their fertility. However, our study shows that these mating costs to female fertility have been counteracted through the evolution of an OA-mediated protective system. There has been extensive research on oxidative stress and its detrimental impact on male fertility.<sup>47</sup> Similarly, substantial research has been devoted to associating the antioxidative capability of mated females with the protective effects of male sperms.<sup>2,51,52</sup> Our finding that the anti-ROS effect of OA protects the reproductive tract of mated hermaphrodites provides new insights into ROS-associated infertility in females.

OA is an important adrenergic neurotransmitter/neurohormone. Like norepinephrine in mammals, OA regulates behavior and metabolism and is often considered the primary "fight-or-flight" stress hormone in invertebrates. In mammals, OA exists in trace amounts, but its biological function has yet to be established.<sup>53</sup>

Nevertheless, OA has existed as a pharmaceutical product for many years, and, though banned by the World Anti-Doping Agency (WADA) for use in competition, it is still found in some dietary supplements due to antioxidant properties and minor fat-burning effects.<sup>54,55</sup> This antioxidative function has only been assessed in a few studies on insects and nematodes. In brown planthoppers *Nilaparvata lugens*, paraquat stimulates the expression of an OA receptor, endowing these insects with enhanced resistance to paraquat-induced oxidative stress.<sup>56</sup> Similarly, in *C. elegans*, paraquat-induced oxidative stress elevates OA levels, which signals to the transcription factor DAF-16/FOXO to induce the expression of antioxidant factors.<sup>57</sup> Here, we have shown that OA upregulates antioxidant GSH synthesis to protect ovulation and fertility from ROS-induced damage in the spermathecae. To exert this effect, OA adopts a unique signaling pathway consisting of the spermatheca-enriched receptor SER-3, TPA-1, and the MAPK KGB-1 cascade to transduce the signal to SKN-1/Nrf2, a master regulator that controls both enzymatic and non-enzymatic antioxidant levels.

That OA plays a vital role in female reproduction has been best demonstrated in fruit flies, where it regulates oogenesis, ovulation, sperm storage, and oviposition, among other effects.<sup>58–61</sup> *Drosophila* females require a successful mating event to optimize their reproductive tract for fertilization and to attain a maximal reproductive rate. OA signaling increases the population of germline stem cells upon mating and elicits innervation and remodeling of the oviduct to expand its cellular junctions and luminal space,<sup>62–64</sup> indicating that OA signaling is involved in mating-triggered maturation of the reproductive tract. However, unlike *Drosophila*, *C. elegans* hermaphrodites produce sperms for self-fertility that, under well-fed conditions, gives rise to an ovulation rate similar to mating-based fertility (Figure 2B). Thus, OA appears to be dispensable for gonad maturation in nematodes, which is supported by the *tbh-1* mutant hermaphrodites still producing around 200 self-progenies despite lacking OA. Instead, as demonstrated in our study, OA acts as a primary neurohormone protecting spermathecae against ROS-induced damage to ensure optimal ovulation in mated hermaphrodites and perhaps also in unmated hermaphrodites as OA also improved self-fertility in unmated *tbh-1* hermaphrodites (Figure 1F).

Anatomically, insects share more similarities with mammals than *C. elegans* in terms of their female reproductive tracts, both having ovaries and oviducts where fertilization occurs. Although spermathecae exist in the insect female reproductive tract,<sup>65</sup> they only serve to store male sperm and do not undergo dilation cycles arising from oocyte passage as in *C. elegans*. However, insect oviducts transport oocytes during fertilization, and in some regions its epithelial cells are joined by pleated septate junctions, just like those of *C. elegans* spermathecal bag cells.<sup>50,62</sup> Mated OA-deficient *Drosophila* females are infertile due to oocyte retention but can still lay eggs and produce progeny when transferred to OA-supplemented food,<sup>66</sup> yet it still remains unclear how OA prevents this ovipositional defect. Given the similarities between oviduct and spermatheca in hosting passing oocytes during fertilization, just like our finding that OA protects spermathecae to prevent impaired ovulation, OA may protect oviducts to prevent ovipositional defects.

Specific expression of SKN-1(lax188) in spermathecae prevented impaired ovulation and rescued the suppressed fertility displayed by mated *tbh-1* hermaphrodites. Nevertheless, it failed to enhance mating-promoted fertility to the levels determined for mated N2 hermaphrodites. In contrast, ubiquitously expressed SKN-1(lax188) fully promoted mating-based fertility of *tbh-1* hermaphrodites to N2 levels. These results indicate that, in addition to its protective role in the spermathecae, OA-SKN-1 signaling acts in other tissues to promote optimal mating fertility for sexual reproduction.

In summary, our work establishes a crucial role for OA signaling in counterbalancing a previously unknown mating cost in females to secure cross-offspring production. In addition, we reveal a complete signaling pathway by which OA regulates GSH synthesis to protect against mating-induced ROS and maintain spermathecal function in *C. elegans* hermaphrodites.

### Limitations of the study

A limitation of our study is the delivery of exogenous OA and GSH into worm bodies. Although supplementation of either OA or GSH in culture media could abolish the inhibited fertility in mated *tbh-1* hermaphrodites, neither could fully rescue their mating fertility to the levels in control N2 hermaphrodites. Additional studies are required to overcome this experimental limitation to deliver exogenous OA and GSH.



**STAR★METHODS**

Detailed methods are provided in the online version of this paper and include the following:

- **KEY RESOURCES TABLE**
- **RESOURCE AVAILABILITY**
  - Lead contact
  - Materials availability
  - Data and code availability
- **EXPERIMENTAL MODEL AND SUBJECT DETAILS**
  - Nematode maintenance and transgenic nematode generation
- **METHOD DETAILS**
  - Mating setup and fertility assay
  - Ovulation analysis
  - EDU and ROS staining of live nematodes
  - Viability staining of spermathecal cells
  - Whole-nematode <sup>35</sup>S-methionine labeling and protein analysis
  - Western blotting
  - Laser ablation of individual neurons
  - OA measurement
  - Glutathione measurement
  - Quantitative RT-PCR (qPCR)
- **QUANTIFICATION AND STATISTICAL ANALYSIS**

**SUPPLEMENTAL INFORMATION**

Supplemental information can be found online at <https://doi.org/10.1016/j.isci.2023.106162>.

**ACKNOWLEDGMENTS**

We are grateful to Drs Naoki Hisamoto and Kunihiro Matsumoto at Nagoya University, Japan, for the antibodies against *C. elegans* KGB-1 and its phosphorylated form. We thank Dr. Chih-Yu Lin and Ms. Ting-Hsiang Chang for UPLC-MS/MS parameter optimization and the Metabolomics Core Facility of the Agricultural Biotechnology Research Center at Academia Sinica for technical support.

**AUTHOR CONTRIBUTIONS**

Y.H.L. conceived and designed experiments, supervised the research, analyzed data, and wrote the manuscript. Y.T. and Y.C.L. performed experiments and analyzed data.

**DECLARATION OF INTERESTS**

The authors declare no competing interests.

Received: July 11, 2022

Revised: December 12, 2022

Accepted: February 2, 2023

Published: February 9, 2023

**REFERENCES**

1. Lange, R., Reinhardt, K., Michiels, N.K., and Anthes, N. (2013). Functions, mechanisms, and evolution of traumatic mating. *Biol. Rev.* *88*, 585–601. <https://doi.org/10.1111/bvr.12018>.
2. Reinhardt, K., Anthes, N., and Lange, R. (2015). Copulatory wounding and traumatic insemination. *Cold Spring Harb. Perspect. Biol.* *7*, a017582. <https://doi.org/10.1101/cshperspect.a017582>.
3. Barr, M.M., and Garcia, L.R. (2006). Male mating behavior. In *The C. elegans Research Community, Wormbook*, ed. (WormBook).
4. Woodruff, G.C., Knauss, C.M., Mangel, T.K., and Haag, E.S. (2014). Mating damages the cuticle of *C. elegans* hermaphrodites. *PLoS One* *9*, e104456. <https://doi.org/10.1371/journal.pone.0104456>.
5. Oku, K., Price, T.A.R., and Wedell, N. (2019). Does mating negatively affect female immune defences in insects? *Animal. Biol.* *69*, 117–136. <https://doi.org/10.1163/15707563-20191082>.
6. Santiago-Moreno, J., and Blesbois, E. (2020). Functional aspects of seminal plasma in bird reproduction. *Int. J. Mol. Sci.* *21*, 5664–5680. <https://doi.org/10.1101/cshperspect.a017582>.
7. Wigby, S., Brown, N.C., Allen, S.E., Misra, S., Sitnik, J.L., Sepil, I., Clark, A.G., and Wolfner, M.F. (2020). The *Drosophila* seminal proteome and its role in postcopulatory sexual selection. *Phil. Trans. R. Soc. B* *375*, 20200072. <https://doi.org/10.1098/rstb.2020.0072>.
8. Smyth, S.P., Nixon, B., Anderson, A.L., Murray, H.C., Martin, J.H., MacDougall, L.A.,

- Robertson, S.A., Skerrett-Byrne, D.A., and Schjenken, J.E. (2022). Elucidation of the protein composition of mouse seminal vesicle fluid. *Proteomics* 22, e202100227. <https://doi.org/10.1002/ptmic.202100227>.
9. South, A., and Lewis, S.M. (2011). The influence of male ejaculate quantity on female fitness: a meta analysis. *Biol. Rev. Camb. Philos. Soc.* 86, 299–309. <https://doi.org/10.1111/j.1469-185X.2010.00145.x>.
  10. Sirot, L.K., Wong, A., Chapman, T., and Wolfner, M.F. (2015). Sexual conflict and seminal fluid proteins. *Cold Spring Harb. Perspect. Biol.* 7, a017533. <https://doi.org/10.1101/cshperspect.a017533>.
  11. Schjenken, J.E., and Robertson, S.A. (2020). The female response to seminal fluid. *Physiol. Rev.* 100, 1077–1117. <https://doi.org/10.1152/physrev.00013.2018>.
  12. Billeter, J.C., and Wolfner, M.F. (2018). Chemical cues that guide female reproduction in *Drosophila melanogaster*. *J. Chem. Ecol.* 44, 750–769. <https://doi.org/10.1007/s10886-018-0947-z>.
  13. Chapman, T., Liddle, L.F., Kalb, J.M., Wolfner, M.F., and Partridge, L. (1995). Cost of mating in *Drosophila melanogaster* females is mediated by male accessory gland products. *Nature* 373, 241–244. <https://doi.org/10.1038/373241a0>.
  14. Ram, K.R., and Wolfner, M.F. (2007). Sustained post-mating response in *Drosophila melanogaster* requires multiple seminal fluid proteins. *PLoS Genet.* 3, e238. <https://doi.org/10.1371/journal.pgen.0030238>.
  15. Chapman, T., Arnqvist, G., Bangham, J., and Rowe, L. (2003). Sexual conflict. *Trends Ecol. Evol.* 18, 41–47. [https://doi.org/10.1016/S0169-5347\(02\)00004-6](https://doi.org/10.1016/S0169-5347(02)00004-6).
  16. Hollis, B., Koppik, M., Wensing, K.U., Ruhmann, H., Genzoni, E., Erkosar, B., Kaweck, T.J., Fricke, C., and Keller, L. (2019). Sexual conflict drives male manipulation of female postmating responses in *Drosophila melanogaster*. *Proc. Natl. Acad. Sci. USA* 116, 8437–8444. <https://doi.org/10.1073/pnas.1821386116>.
  17. Adefuye, A.O., Adeola, H.A., Sales, K.J., and Katz, A.A. (2016). Seminal fluid-mediated inflammation in physiology and pathology of the female reproductive tract. *J. Immunol. Res.* 2016, 9707252. <https://doi.org/10.1155/2016/9707252>.
  18. Fowler, K., and Partridge, L. (1989). A cost of mating in female fruitflies. *Nature* 338, 760–761.
  19. Morrow, E.H., and Arnqvist, G. (2003). Costly traumatic insemination and a female counter-adaptation in bed bugs. *Proc. R. Soc. B* 207, 2377–2381. <https://doi.org/10.1098/rspb.2003.2514>.
  20. Backhouse, A., Salt, S.M., and Cameron, T.C. (2012). Multiple mating in the traumatically inseminating Warehouse pirate bug, *Xylocoris flavipes*: effects on fecundity and longevity. *Biol. Lett.* 8, 706–709. <https://doi.org/10.1098/rsbl.2012.0091>.
  21. Ajila, H.E.V., Michaud, J.P., Abdelwahab, A.H., Kuchta, S.V., and Stowe, H.E. (2019). How efficient is fertilization by traumatic insemination in *Orius insidiosus* (Hemiptera:Anthorcorididae)? *J. Eco. Entomol.* 112, 1618–1622. <https://doi.org/10.1093/jee/toz061>.
  22. Herman, R.K. (2015). Introduction to sex determination. *Wormbook*. In *The C. elegans Research Community. WormBook*.
  23. Sternberg, P.W. (2005). Vulval development. *Wormbook*. In *The C. elegans Research Community. WormBook*.
  24. Roeder, T. (2005). Tyramine and octopamine: ruling behavior and metabolism. *Annu. Rev. Entomol.* 50, 447–477. <https://doi.org/10.1146/annurev.ento.50.071803.130404>.
  25. Alkema, M.J., Hunter-Ensor, M., Ringstad, N., and Horvitz, H.R. (2005). Tyramine functions independently of octopamine in the *Caenorhabditis elegans* nervous system. *Neuron* 46, 247–260. <https://doi.org/10.1016/j.neuron.2005.02.024>.
  26. Yoshida, M., Oami, E., Wang, M., Ishiura, S., and Suo, S. (2014). Nonredundant function of two highly homologous octopamine receptors in food-deprivation-mediated signaling in *Caenorhabditis elegans*. *J. Neurosci. Res.* 92, 671–678. <https://doi.org/10.1002/jnr.23345>.
  27. Sellegounder, D., Yuan, C.-H., Wibisono, P., Liu, Y., and Sun, J. (2018). Octopaminergic signaling mediates neural regulation of innate immunity in *Caenorhabditis elegans*. *Host Microbe Biol.* 9, 016455–e1718. <https://doi.org/10.1128/mBio.01645-18>.
  28. Suo, S., Kimura, Y., and Van Tol, H.H. (2006). Starvation induces cAMP response element-binding protein-dependent gene expression through octopamine–Gq signaling in *Caenorhabditis elegans*. *J. Neurosci.* 26, 10082–10090. <https://doi.org/10.1523/JNEUROSCI.0819-06.2006>.
  29. Chen, Y., Granger, A.J., Tran, T., Saulnier, J.L., Kirkwood, A., and Sabatini, B.L. (2017). Endogenous Gαq-coupled neuromodulator receptors activate protein kinase A. *Neuron* 96, 1070–1083. <https://doi.org/10.1016/j.neuron.2017.10.023>.
  30. Mizuno, T., Hisamoto, N., Terada, T., Kondo, T., Adachi, M., Nishida, E., Kim, D.H., Ausubel, F.M., and Matsumoto, K. (2004). The *Caenorhabditis elegans* MAPK phosphatase VHP-1 mediates a novel JNK-like signaling pathway in stress response. *EMBO J.* 23, 2226–2234. <https://doi.org/10.1038/sj.emboj.7600226>.
  31. Gerke, P., Keshet, A., Mertenskötter, A., and Paul, R.J. (2014). The JNK-like MAPK KGB-1 of *Caenorhabditis elegans* promotes reproduction, lifespan, and gene expressions for protein biosynthesis and germline homeostasis but interferes with hyperosmotic stress tolerance. *Cell. Physiol. Biochem.* 34, 1951–1973. <https://doi.org/10.1159/000366392>.
  32. Karin, M., Liu, Z., and Zandi, E. (1997). AP-1 function and regulation. *Curr. Opin. Cell Biol.* 9, 240–246. [https://doi.org/10.1016/s0955-0674\(97\)80068-3](https://doi.org/10.1016/s0955-0674(97)80068-3).
  33. Uno, M., Honjoh, S., Matsuda, M., Hoshikawa, H., Kishimoto, S., Yamamoto, T., Ebisuya, M., Yamamoto, T., Matsumoto, K., and Nishida, E. (2013). A fasting-responsive signaling pathway that extends life span in *C. elegans*. *Cell Rep.* 3, 79–91. <https://doi.org/10.1016/j.celrep.2012.12.018>.
  34. Inoue, H., Hisamoto, N., An, J.H., Oliveira, R.P., Nishida, E., Blackwell, T.K., and Matsumoto, K. (2005). The *C. elegans* p38 MAPK pathway regulates nuclear localization of the transcription factor SKN-1 in oxidative stress response. *Genes Dev.* 19, 2278–2283. <https://doi.org/10.1101/gad.1324805>.
  35. Tullet, J.M.A., Green, J.W., Au, C., Benedetto, A., Thompson, M.A., Clark, E., Gilliat, A.F., Young, A., Schmeisser, K., and Gems, D. (2017). The SKN-1/Nrf2 transcription factor can protect against oxidative stress and increase lifespan in *C. elegans* by distinct mechanisms. *Aging Cell* 16, 1191–1194. <https://doi.org/10.1111/ace1.12627>.
  36. Paek, J., Lo, J.Y., Narasimhan, S.D., Nguyen, T.N., Glover-Cutter, K., Robida-Stubbs, S., Suzuki, T., Yamamoto, M., Blackwell, T.K., and Curran, S.P. (2012). Mitochondrial SKN-1/Nrf mediates a conserved starvation response. *Cell Metabol.* 16, 526–537. <https://doi.org/10.1016/j.cmet.2012.09.007>.
  37. Chi, W., and Reinke, V. (2009). DPL-1 (DP) acts in the germ line to coordinate ovulation and fertilization in *C. elegans*. *Mech. Dev.* 126, 406–416. <https://doi.org/10.1016/j.mod.2009.01.008>.
  38. Blackwell, T.K., Steinbaugh, M.J., Hourihan, J.M., Ewald, C.Y., and Isik, M. (2015). SKN-1/Nrf, stress responses, and aging in *Caenorhabditis elegans*. *Free Radic. Biol. Med.* 88, 290–301. <https://doi.org/10.1016/j.freeradbiomed.2015.06.008>.
  39. An, J.H., and Blackwell, T.K. (2003). SKN-1 links *C. elegans* mesodermal specification to a conserved oxidative stress response. *Genes Dev.* 17, 1882–1893. <https://doi.org/10.1101/gad.1107803>.
  40. Tullet, J.M.A., Hertweck, M., An, J.H., Baker, J., Hwang, J.Y., Liu, S., Oliveira, R.P., Baumeister, R., and Blackwell, T.K. (2008). Direct inhibition of the longevity-promoting factor SKN-1 by insulin-like signaling in *C. elegans*. *Cell* 132, 1025–1038. <https://doi.org/10.1016/j.cell.2008.01.030>.
  41. Park, S.K., Tedesco, P.M., and Johnson, T.E. (2009). Oxidative stress and longevity in *Caenorhabditis elegans* as mediated by SKN-1. *Aging Cell* 8, 258–269. <https://doi.org/10.1111/j.1474-9726.2009.00473.x>.
  42. Lu, S.C. (2013). Glutathione synthesis. *Biochim. Biophys. Acta* 1830, 3143–3153. <https://doi.org/10.1016/j.bbagen.2012.09.008>.
  43. Ferguson, G.D., and Bridge, W.J. (2019). The glutathione system and the related thiol

- network in *Caenorhabditis elegans*. *Redox Biol.* 24, 101171. <https://doi.org/10.1016/j.redox.2019.101171>.
44. Papp, D., Csermely, P., and Söti, C. (2012). A role for SKN-1/Nrf in pathogen resistance and immunosenescence in *Caenorhabditis elegans*. *PLoS Pathog.* 8, e1002673. <https://doi.org/10.1371/journal.ppat.1002673>.
  45. Khan, A.U., and Wilson, T. (1995). Reactive oxygen species as cellular messengers. *Chem & Biol.* 2, 437–444. [https://doi.org/10.1016/1074-5521\(95\)90259-7](https://doi.org/10.1016/1074-5521(95)90259-7).
  46. Aitken, R.J., and Drevet, J.R. (2020). The importance of oxidative stress in determining the functionality of mammalian spermatozoa: a two-edged sword. *Antioxidants* 9, 111. <https://doi.org/10.3390/antiox9020111>.
  47. Aitken, R.J. (2020). Impact of oxidative stress on male and female germ cells: implications for fertility. *Reproduction* 159, R189–R201. <https://doi.org/10.1530/REP-19-0452>.
  48. Koppers, A.J., Garg, M.L., and Aitken, R.J. (2010). Stimulation of mitochondrial reactive oxygen species production by unesterified, unsaturated fatty acids in defective human spermatozoa. *Free Radical Biol. Med.* 48, 112–119. <https://doi.org/10.1016/j.freeradbiomed.2009.10.033>.
  49. LaMunyon, C.W., and Ward, S. (1997). Increased competitiveness of nematode sperm bearing the male X chromosome. *Proc. Natl. Acad. Sci. USA* 94, 185–189. <https://doi.org/10.1073/pnas.94.1.185>.
  50. Lints, R., and Hall, D.H. (2009). Reproductive system, somatic gonad. In *WormAtlas*.
  51. Heifetz, Y., and Rivlin, P.K. (2010). Beyond the mouse model: using *Drosophila* as a model for sperm interaction with the female reproductive tract. *Theriogenology* 73, 723–739. <https://doi.org/10.1016/j.theriogenology.2009.11.001>.
  52. Gonzalez, A.N., Ing, N., and Rangel, J. (2018). Upregulation of antioxidant genes in the spermathecae of honey bee (*Apis mellifera*) queens after mating. *Apidologie* 49, 224–234. <https://doi.org/10.1007/s13592-017-0546-y>.
  53. Kakimoto, Y., and Armstrong, M.D. (1962). On the identification of octopamine in mammals. *J. Biol. Chem.* 237, 422–427.
  54. Vesali, M., Azarbayjani, M.A., and Peeri, M. (2021). Effect of aerobic training and octopamine supplementation on the expression of octopamine receptors in the visceral adipose tissue of rats exposed to deep fried oils. *Gene Cell Tissue E*, e110290. <https://doi.org/10.5812/gct.110290>.
  55. Ziaie Bigdeli, T., Peeri, M., Azarbayjani, M.A., and Farzanegi, P. (2021). Synergic effects of endurance training and octopamine on oxidative stress in the cerebellum of male rats treated with deep frying oils. *RJMS* 28, 125–134. <http://rjms.iums.ac.ir/article-1-6696-en.html>.
  56. Zhang, Y.J., Jiang, L., Ahamd, S., Chen, Y., Zhang, J.Y., Stanley, D., Miao, H., and Ge, L.Q. (2022). The octopamine receptor, OA2B2, modulates stress resistance and reproduction in *Nilaparvata lugens* Stål (Hemiptera: Delphacidae). *Insect Mol. Biol.* 31, 33–48. <https://doi.org/10.1111/imb.12736>.
  57. Hoshikawa, H., Uno, M., Honjoh, S., and Nishida, E. (2017). Octopamine enhances oxidative stress Resistance through the fasting-responsive transcription factor DAF-16/FOXO in *C. elegans*. *Gene Cell.* 22, 210–219. <https://doi.org/10.1111/gtc.12469>.
  58. Monastirioti, M. (2003). Distinct octopamine cell population residing in the CNS abdominal ganglion controls ovulation in *Drosophila melanogaster*. *Dev. Biol.* 264, 38–49. <https://doi.org/10.1016/j.ydbio.2003.07.019>.
  59. Deady, L.D., and Sun, J. (2015). A follicle rupture assay reveals an essential role for follicular adrenergic signaling in *Drosophila* ovulation. *PLoS Genet.* 11, e1005604. <https://doi.org/10.1371/journal.pgen.1005604>.
  60. Li, F., Li, K., Wu, L.-J., Fan, Y.-L., and Liu, T.-X. (2020). Role of biogenic amines in oviposition by the Diamondback moth, *Plutella xylostella* L. *Front. Physiol.* 11, 475. <https://doi.org/10.3389/fphys.2020.00475>.
  61. White, M.A., Chen, D.S., and Wolfner, M.F. (2021). She's got nerve: roles of octopamine in insect female reproduction. *J. Neurogenet.* 35, 132–153. <https://doi.org/10.1080/01677063.2020.1868457>.
  62. Kapelnikov, A., Rivlin, P.K., Hoy, R.R., and Heifetz, Y. (2008). Tissue remodeling: a mating-induced differentiation program for the *Drosophila* oviduct. *BMC Dev. Biol.* 8, 114. <https://doi.org/10.1186/1471-213X-8-114>.
  63. Heifetz, Y., Lindner, M., Garini, Y., and Wolfner, M.F. (2014). Mating regulates neuromodulator ensembles at nerve termini innervating the *Drosophila* reproductive tract. *Curr. Biol.* 24, 731–737. <https://doi.org/10.1016/j.cub.2014.02.042>.
  64. Yoshinari, Y., Ameku, T., Kondo, S., Tanimoto, H., Kuraishi, T., Shimada-Niwa, Y., and Niwa, R. (2020). Neuronal octopamine signaling regulates mating-induced germline stem cell increase in female *Drosophila melanogaster*. *Elife* 9, e57101. <https://doi.org/10.7554/eLife.57101>.
  65. Hoffmann, K.H. (1995). Oogenesis and the female reproductive system. In *Insect Reproduction*, S.R. Leather and J. Hardie, eds. (CRC Press), pp. 1–32.
  66. Monastirioti, M., Linn, C.E., Jr., and White, K. (1996). Characterization of *Drosophila* tyramine beta-hydroxylase gene and isolation of mutant flies lacking octopamine. *J. Neurosci.* 16, 3900–3911. <https://doi.org/10.1523/JNEUROSCI.16-12-03900.1996>.

## STAR★METHODS

### KEY RESOURCES TABLE

REAGENT or RESOURCE	SOURCE	IDENTIFIER
<b>Antibodies</b>		
Rabbit polyclonal anti-KGB-1	Generated in lab	Mizuno et al. <sup>30</sup>
Rabbit polyclonal anti-phospho-KGB-1	Generated in lab	Mizuno et al. <sup>30</sup>
<b>Chemicals</b>		
L-Glutathione reduced	Sigma-Aldrich	G4251
$\alpha$ -Lipoic Acid	Sigma-Aldrich	T5625
Melatonin	Sigma-Aldrich	M5250
Octopamine hydrochloride	Sigma-Aldrich	O0250
Sodium L-Ascorbate	Sigma-Aldrich	A4034
<b>Critical commercial assays</b>		
Click-iT™ EdU Cell Proliferation Kit for Imaging	ThermoFisher	C10337
Glutathione colometric assay kit	BioVision	K261
LIVE/DEAD Sperm viability kit	Molecular Probe	L7011
<b>Experimental models: <i>C. elegans</i> strains</b>		
AQ866 ser-4(ok512)	CGC	N/A
BS3383 pmk-3(ok169)	CGC	N/A
CB1111 cat-1(e1111)	CGC	N/A
CB1112 cat-2(e1112)	CGC	N/A
CB1141 cat-4(e1141)	CGC	N/A
CX12800 ser-3(ad1774)	CGC	N/A
CX13079 octr-1(ok371)	CGC	N/A
CZ4213 mkk-4(ju91)	CGC	N/A
DA2109 ser-7(tm1325) ser-1(ok345)	CGC	N/A
EJ255 mek-2(q484) l; sDp2 (l; f)	CGC	N/A
FK171 mek-1(ks54) sek-1(qd127)	CGC	N/A
FK312 sma-5(n678)	CGC	N/A
IK130 pkc-1(nj3)	CGC	N/A
JT73 itr-1(sa73)	CGC	N/A
KB3 kgb-1(um3)	CGC	N/A
KK1228 pkc-3(it309[GFP::pkc-3])	CGC	N/A
KP4 glr-1(n2461)	CGC	N/A
KU12 dlk-1(km12)	CGC	N/A
KU2 jkk-1(km2)	CGC	N/A
KU25 pmk-1(km25)	CGC	N/A
KU4 sek-1(km4)	CGC	N/A
LX645 dop-1(vs100)	CGC	N/A
MJ563 tpa-1(k530)	CGC	N/A
MQ1766 sod-2(ok1030) sod-5 (tm1146) sod-1(tm783) sod-4(gk101) sod-3(tm760)	CGC	N/A
MT1083 egl-8(n488)	CGC	N/A
MT13113 tdc-1(n3419)	CGC	N/A

(Continued on next page)

*Continued*

REAGENT or RESOURCE	SOURCE	IDENTIFIER
MT13544 ceh-30(n4289)	CGC	N/A
MT1434 egl-30(n686)	CGC	N/A
MT15434 tph-1(mg280)	CGC	N/A
MT5044 ces-2(n732)	CGC	N/A
MT7988 bas-1(ad446)	CGC	N/A
MT9455 tbh-1(n3247)	CGC	N/A
MT9971 nls107[tbh-1::GFP + lin-15(+)]	CGC	N/A
N2 wild-type	CGC	N/A
NL737 mut-2(r459) I; mek-1(pk97)	CGC	N/A
OH313 ser-2(pk1357)	CGC	N/A
PJ1077 let-60(ga89); lws16	CGC	N/A
PS4112 plc-1(rx1); kfEx2	CGC	N/A
PS4886 plc-3(tm1340)/mln1 [mls14 dpy-10(e128)]	CGC	N/A
PY1589 cmk-1(oy21)	CGC	N/A
QV225 skn-1(zj15)	CGC	N/A
RB1034 gskl-2(gska-3)(ok970)	CGC	N/A
RB1197 ctl-1(ok1242)	CGC	N/A
RB1287 sek-6(ok1386)	CGC	N/A
RB1437 skop-1(ok1640)	CGC	N/A
RB1496 plc-2(ok1761)	CGC	N/A
RB1627 pll-1(ok2003)	CGC	N/A
RB1653 ctl-3(ok2042)	CGC	N/A
RB1808 glr-2(ok2342)	CGC	N/A
RB1908 mlk-1(ok2471)	CGC	N/A
RB2037 dkf-1(ok2695)	CGC	N/A
RB2277 ser-5(ok3087)	CGC	N/A
RB582 mpk-2(ok219)	CGC	N/A
SD939 mpk-1(ga111) unc-79(e1068)	CGC	N/A
SP1745 dyf-5(mn400)	CGC	N/A
SPC167 skn-1(lax120); dvls19	CGC	N/A
SPC168 skn-1(lax188); dvls19	CGC	N/A
tm1521 plc-4(tm1521)	NBRP	N/A
tm1990 gpx-7(tm1990)	NBRP	N/A
tm2024 gpx-5(tm2024)	NBRP	N/A
tm2100 gpx-1(tm2100)	NBRP	N/A
tm2108 gpx-8(tm2108)	NBRP	N/A
tm2111 gpx-4(tm2111)	NBRP	N/A
tm2139 gpx-3(tm2139)	NBRP	N/A
tm2535 gpx-6(tm2535)	NBRP	N/A
tm2895 gpx-2(tm2895)	NBRP	N/A
tm2146 ser-6(tm2146)	NBRP	N/A
tm3294 gst-4(tm3294)	NBRP	N/A
tm4076 dkf-2(tm4076)	NBRP	N/A
tm4887 gst-10 (tm4887)	NBRP	N/A
tm4392 atf-7(tm4392)	NBRP	N/A
VC1184 jun-1(gk551)	CGC	N/A

(Continued on next page)

**Continued**

REAGENT or RESOURCE	SOURCE	IDENTIFIER
VC125 tyra-3(ok325)	CGC	N/A
VC127 pkc-2(ok328)	CGC	N/A
VC175 sod-4(gk101)	CGC	N/A
VC2695 mapk-15(gk1234)	CGC	N/A
VC390 nsy-1(ok593)	CGC	N/A
VC754 ctl-2(ok1137)	CGC	N/A
VC8 jnk-1(gk7)	CGC	N/A
VC822 kgb-2(gk361)	CGC	N/A
VZ12 trxr-2(tm2047)	CGC	N/A
WM92 mom-4(ne1539)	CGC	N/A
YHR01 tbh-1(n3247) skn-1(lax188)	This study	N/A
YHR02 kgb-1(lum3) skn-1(lax188)	This study	N/A
YHR03 ser-3(ad1774) ser-6(tm2146)	This study	N/A
YHR04 ser-3(ad1774) octr-1(ok371)	This study	N/A
YHR05 ser-6(tm2146) octr-1(ok371)	This study	N/A
YT17 crh-1(tz2)	CGC	N/A
<b>Oligonucleotides</b>		
gpx-1 qPCR primer-1 GAATATCGATTTACACGATG	This study	N/A
gpx-1 qPCR primer-2 CGGATTACAAAGGAAAAGTTC	This study	N/A
gpx-6 qPCR primer-1 GAATGTGAGTATCTTCCAACC	This study	N/A
gpx-6 qPCR primer-2 AAGCAGTTATACATATGCGCC	This study	N/A
gpx-7 qPCR primer-1 CCTGAAATCCAAATTGGTTGC	This study	N/A
gpx-7 qPCR primer-2 CAAATACAGCGGACTTGTTC	This study	N/A
gcs-1 qPCR primer-1 CTTTATTTTCGAAACGAGCAAC	This study	N/A
gcs-1 qPCR primer-2 GAGATGGCATCCATCTTTTTTC	This study	N/A
gsr-1 qPCR primer-1 CGTTACGATAAGGTTCTCC	This study	N/A
gsr-1 qPCR primer-2 TCTGAACCTTTTCGATGACTC	This study	N/A
gss-1 qPCR primer-1 GATTGGGCTCATGCTAATGG	This study	N/A
gss-1 qPCR primer-2 TGGGCTTTGACTTTCTCAAG	This study	N/A
gst-44 qPCR primer-1 GATTCCTGAGTACTTGGATG	This study	N/A
gst-44 qPCR primer-2 GCCAATAGACACGTTGAAAG	This study	N/A
sgo-1 qPCR primer-1 TGCACCTATGCTCATTGCTC	This study	N/A
sgo-1 qPCR primer-2 TTGGTTCATCATGCTTTCCA	This study	N/A
skn-1 qPCR primer-1 GCTCCAGCAGCTGTCAACT	This study	N/A
skn-1 qPCR primer-2 GATGTTGGGAACACTCTGTC	This study	N/A
sod-1 qPCR primer-1 GATTTTTCCGCAGGTCGAAG	This study	N/A
sod-1 qPCR primer-2 ACGGATCTCGGATTTTGTC	This study	N/A
kgb-1 genotyping primer-1 CTGTAAGATTTGAGATGCATG	This study	N/A
kgb-1 genotyping primer-2 CACGCCGTACGTATCCGCATG	This study	N/A
kgb-1 genotyping primer-3 GACTTGTTAGAGACTAATAGACG	This study	N/A
skn-1(lax188) genotyping primer-1 CCTATTGCGTAAGTACATGG	This study	N/A
skn-1(lax188) genotyping primer-2 CTTCATATCGAGCATTCTC	This study	N/A
skn-1(lax188) genotyping primer-3 CTTCATATCGAGCATTCTT	This study	N/A
tbh-1 genotyping primer-1 GTGACTTAGATGATTAATTCATGAT	This study	N/A
tbh-1 genotyping primer-2 CACACCTGAGTTGTCCGGTTAC	This study	N/A
tbh-1 genotyping primer-3 CAGTTGAATCTGGTATGGATTTTGAG	This study	N/A

(Continued on next page)

**Continued**

REAGENT or RESOURCE	SOURCE	IDENTIFIER
Recombinant DNA		
pPD95.75-sth-1p::skn-1(lax188)	This study	N/A
Software and algorithms		
AxioVision	Fisher Science	<a href="https://www.fishersci.pt">https://www.fishersci.pt</a>
MetaMorph	Molecular Device	<a href="https://www.moleculardevice.com">https://www.moleculardevice.com</a>
ImageJ	NIH	<a href="https://ImageJ.nih.gov">https://ImageJ.nih.gov</a>
Imaris 9.8	Oxford Instruments	<a href="https://imaris.oxinst.com">https://imaris.oxinst.com</a>

**RESOURCE AVAILABILITY****Lead contact**

Further information and requests for resources and reagents should be directed to and will be fulfilled by the lead contact, Ying-Hue Lee ([yinghue@gate.sinica.edu.tw](mailto:yinghue@gate.sinica.edu.tw)).

**Materials availability**

Worm strains generated from this study are available from the [lead contact](#) upon request.

**Data and code availability**

Data reported in this paper will be shared by the [lead contact](#) upon request.

No original code was used in this study.

Any additional information required to reanalyze the data reported in this paper is available from the [lead contact](#) upon request.

**EXPERIMENTAL MODEL AND SUBJECT DETAILS****Nematode maintenance and transgenic nematode generation**

Nematodes were maintained on agar plates covered with an OP50 bacterial lawn at 15°C using standard techniques. Male populations of *C. elegans* N2 nematodes were maintained by mating males and hermaphrodites in every generation. To transiently express the indicated transgenes in specific tissues, a tissue-specific promoter and the coding sequences of each gene tagged with GFP at the C-terminal were subcloned into the vector pPD95.75 and used for DNA microinjection (100 ng/μL) to generate nematodes carrying the extra-chromosomal transgene array. Expression of a transgene in tissues was verified by the presence of a GFP signal in the designated tissues.

**METHOD DETAILS****Mating setup and fertility assay**

Late L4 N2 hermaphrodites, i.e., within 6 h of the adult stage, were placed overnight at 22°C in a mating agar plate individually or in groups with 3-fold the number of Day 1 young adult males. Then, the hermaphrodites were placed separately in a well of a 12-well agar plate and transferred daily to a new well until they no longer laid eggs. The offspring produced daily were allowed to grow at 22°C until their sex could be easily identified and they were counted to ascertain mating success and determine offspring number.

**Ovulation analysis**

Live-imaging was employed to determine ovulation rates. To image ovulation, hermaphrodites were immobilized on 4% agar pads with an anesthetic (5 mM Levamisole hydrochloride). DIC images were captured using an Andor Revolution WD Spinning Disk confocal microscope and an Andor CCD system. Images were captured every 30 s across a 120-min session. Ovulation rate was calculated as the number of successfully ovulated oocytes per gonad over the 120-min session. The time oocytes spent in spermathecae was also calculated. Oocytes that stalled in spermathecae during the 120-min session were assigned a time spent in spermathecae of 120 min. At least 20 gonads were examined for each nematode strain.



### EDU and ROS staining of live nematodes

For EdU-labeling of mitotic germ cells, Day-1 mated hermaphrodites were incubated on an agar plate in PBS with 100  $\mu$ M EdU (Click-iT EdU Imaging Kit, Invitrogen) and bacterial food for the indicated period. Gonads were dissected, fixed and mounted onto slides, before being incubated in freshly-prepared Click-IT reaction cocktail for 30 min in the dark at room temperature. After incubation, the gonads were washed in PBS for 5 min and stained in Hoechst 33,342 (1  $\mu$ g/mL), before being visualized under fluorescence microscopy for EdU and nuclei signals. For ROS staining, nematodes were washed with PBS and stained in 10-15  $\mu$ L ROS reagent (CellROX orange, Molecular Probes, 2.5  $\mu$ M in PBS, DMSO 0.2%) for 80 min in the dark. After staining, the nematodes were washed in PBS three times, each for 10 min, before being transferred to 2  $\mu$ L of 5 mM Levamisole hydrochloride on a slide and undergoing fluorescence microscopy at 561 nm.

### Viability staining of spermathecal cells

Spermathecae of Day-1 hermaphrodites were stained using a Live/Dead sperm viability assay kit (Molecular Probes). Briefly, spermathecae were dissected and stained in SYBR 14 solution for 5 min at room temperature. Then, propidium iodide and Hoechst 33,342 solutions were added for further staining for another 5 min before being subjected to microscopy imaging.

### Whole-nematode <sup>35</sup>S-methionine labeling and protein analysis

One to two hundred nematodes were washed three times with PBS, transferred to a well of a 12-well microplate, and incubated at 22 C in 0.5 mL PBS containing 50  $\mu$ Ci L-<sup>35</sup>S-methionine (PerkinElmer) for 3 h. The nematodes were then washed with PBS and snap-frozen in liquid nitrogen for protein extraction. Protein extracts were subjected to 10% SDS-PAGE, before being transferred to a PVDF membrane (Millipore, IPVH00010) and exposed to an X-ray film. Coomassie blue was used to stain the blot and assess loading of protein samples.

### Western blotting

Nematodes were collected, washed several times with PBS, and stored at  $-80^{\circ}$ C until analysis. Frozen nematodes were homogenized with RIPA buffer containing protease inhibitor cocktail. Protein concentrations were determined using a DC protein assay (Bio-Rad). Protein (5  $\mu$ g) from each sample was resolved via 10% SDS-PAGE, transferred to a PVDF membrane (Millipore, IPVH00010), blotted with antibodies against KGB-1 and its phosphorylated form<sup>30</sup> using the Can Get Signal system (Toyobo), and finally detected with an ECL system (Lab Frontier). The blot was stained with Coomassie blue to assess loading of protein samples.

### Laser ablation of individual neurons

MT9971 hermaphrodites carrying a GFP transgene driven by a *tbh-1* promoter were used for the laser ablation experiments. Laser ablation was carried out at the L4 stage. Hermaphrodites were placed on a 4% agar pad with an anesthetic (5 mM Levamisole hydrochloride) and received a laser microbeam focused on the fluorescent neurons through a microscope objective (Chameleon 630-1040 nm laser; 100X/1.47 Plan Apochromate/Zeiss LSM 980 Inverted confocal microscope; Zen 3.2 Blue software). Mock hermaphrodites underwent the same treatment protocol as the ablated hermaphrodites, except they were not subjected to the laser microbeam. Abolition of fluorescent signal upon ablation was confirmed 1 day later and continuously monitored during the experimental period.

### OA measurement

An Ultra-Performance Liquid Chromatography (UPLC) system (ACQUITY UPLC, Waters) was used to measure OA samples. Day 1 adult hermaphrodites (n = 500) were prepared for OA measurement, as described previously (Alkema et al., 2005). Samples were injected into an ACQUITY UPLC BEH C18 column (1.7  $\mu$ m particle size, 2.1  $\times$  50 mm) coupled to a Waters Xevo TQ-XS triple quadrupole mass spectrometer (Waters). Characteristic MS transitions were monitored using positive multiple reaction monitoring (MRM) mode for octopamine (*m/z*, 136 > 91). Data acquisition and processing were performed using MassLynx version 4.2 and TargetLynx software (Waters Corp.). OA levels were calculated from the peak areas (Figure S1B) and the standard peaks.

### Glutathione measurement

Day 1 adult hermaphrodites ( $n = 500$ ) were collected, washed with PBS, and homogenized in 40  $\mu\text{L}$  Glutathione Buffer. A Glutathione Colorimetric Assay Kit (BioVision) was applied to samples to quantify total and reduced glutathione levels according to the manufacturer's instructions. Protein levels were quantified using a DC Protein Assay Kit (BioRad).

### Quantitative RT-PCR (qPCR)

Each primer pair was checked for its melting curve before being used for qPCR. qPCR was performed in the presence of SYBR Green using a QuantStudio 12K Flex Real-Time PCR System (Applied Biosystems). Optimization of reactions was performed according to the manufacturer's instructions. The expression levels of *sgo-1* were used to calibrate the expression of other genes in each sample. Relative quantification was computed as the threshold number of cycles of a target gene relative to the endogenous control *sgo-1* gene.

### QUANTIFICATION AND STATISTICAL ANALYSIS

Results are presented as mean  $\pm$  SD ( $M \pm SD$ ). Two-tailed Student's *t*-tests were used for statistical analysis.  $p < 0.01$  was considered statistically significant.